PLUMAGE BALANCES CAMOUFLAGE AND THERMOREGULATION IN HORNED LARKS (*EREMOPHILA ALPESTRIS*)

Nicholas A. Mason[1,2], Eric A. Riddell[1,3], Faye G. Romero[1], Carla Cicero[1], Rauri C.K. Bowie[1,4]

[1] Museum of Vertebrate Zoology, University of California, Berkeley, California, USA

[2] Museum of Natural Science and Department of Biological Sciences, Louisiana State University, Baton Rouge, Louisiana, USA

[3] Iowa State University, Department of Ecology, Evolution, and Organismal Biology, Ames, Iowa, USA

[4] Department of Integrative Biology, University of California, Berkeley, California, USA

*Corresponding author: mason@lsu.edu

ORCIDs: Nicholas A. Mason (0000-0002-5266-463X), Eric A. Riddell (0000-0002-4229-4911), Faye G. Romero (0000-0002-5415-1539), Carla Cicero (0000-0002-6282-2339), Rauri C.K. Bowie (0000-0001-8328-6021)

Keywords: Alaudidae, background matching, crypsis, ecogeographic rules, near-infrared, physiology

Short Title: Camouflage and thermoregulation in Horned Larks

Word count: 12,246

Article type: E-article for submission to *American Naturalist*

Submission contents: main text, five figures, two tables, supplementary information

Abstract

Animal coloration serves many biological functions and must therefore balance potentially competing selective pressures. For example, many animals have camouflage in which coloration matches the visual background that predators scan for prey. However, different colors reflect different amounts of solar radiation and may therefore have thermoregulatory implications as well. In this study, we examined geographic variation in dorsal patterning, coloration, and solar reflectance among Horned Larks (*Eremophila alpestris*) of the western United States. We found that plumage brightness was positively associated with soil granularity, aridity, and temperature. Plumage redness—both in terms of saturation (i.e., chroma) and hue—was positively associated with soil redness and temperature, while plumage patterning was positively associated with soil granularity. Together, these plumage-environment associations support both background matching and Gloger's Rule, a widespread ecogeographic pattern in animal coloration. We also constructed thermoregulatory models that estimated cooling benefits provided by solar reflectance profiles of the dorsal plumage of each specimen based on the collection site. We found increased cooling benefits in hotter, more arid environments. Finally, cooling benefits were positively associated with residual brightness, such that individuals that were brighter than expected based on environmental conditions also had higher cooling benefits, suggesting a tradeoff between camouflage and thermoregulation. Together, these data suggest that natural selection has balanced camouflage and thermoregulation in Horned Larks, and illustrates how multiple competing evolutionary pressures may interact to shape geographic variation in adaptive phenotypes.

Introduction

Animal colors and patterns constitute complex phenotypes that are shaped by a wide array of biotic and abiotic processes (Burtt 1981; Vo et al. 2011; Cuthill et al. 2017; Mason and Bowie 2020). For example, some species have bright colors involved in sexual selection via mate choice (Andersson and Simmons 2006; Shultz and Burns 2017), whereas others have cryptic colors and patterns driven by natural selection to avoid visual detection by predators (Cott 1944; Endler 1978). Integumentary features such as hair, scales, or plumage have important roles as a visual modality for signaling or camouflage, but are also involved in maintaining thermal homeostasis in different environments due to differences in the reflectance of light wavelengths from solar radiation (Walsberg 1983; Wolf and Walsberg 2000; Rogalla et al. 2022). Thus, animal coloration and patterning must balance multiple selective pressures that may conflict or act synergistically to produce multifunctional phenotypes that vary among species and populations across environments (Caro 2017). Among the wide array of biological processes affecting animal colors, camouflage and thermoregulation often have a particularly strong influence on coloration because of their direct impact on survival (Stuart-Fox and Moussalli 2009; Caro and Koneru 2021).

Camouflage includes a suite of physical and behavioral attributes that deter visual detection by predators and is prevalent among various animal lineages, including arthropods (Farkas et al. 2013; Stevens et al. 2014) and vertebrates (Rosenblum et al. 2010; Isaac and Gregory 2013; Boratyński et al. 2017). Also known as background matching, camouflage favors phenotypes that resemble a random sample of brightness, color, and patterning of the visual background against which predators actively scan for

prey (Endler 1978; Merilaita et al. 1999; Michalis et al. 2017). Thermoregulation is also closely tied to coloration (Walsberg 1983) and sometimes favors phenotypes that either conflict with background matching (Smith et al. 2016) or that simultaneously enable thermoregulation and camouflage (Wacker et al. 2016; Gunderson et al. 2022). Many species conform to 'Gloger's Rule,' a widespread ecogeographic pattern that ascribes lighter colors to warmer, more arid environments and darker colors to colder and wetter environments (Gloger 1833; Gaston et al. 2008; Marcondes et al. 2021). A 'complex' version of Gloger's Rule expands this framework to predict more rufous color (typically produced by increased pheomelanin) in more arid environments (Delhey 2019; Marcondes et al. 2020). Recent empirical evidence in support of Gloger's Rule has come from a wide variety of taxa, including various bird lineages (Delhey et al. 2019), primates (Caro et al. 2021), pigs (Newell et al. 2021), and even mushrooms (Krah et al. 2019)—albeit with nuanced associations in certain animal lineages (Marcondes and Brumfield 2020; Marcondes et al. 2021) The patterns underlying Gloger's Rule are thought to be the product of multiple adaptive processes, including camouflage and thermoregulation (Burtt 2004; Delhey et al. 2019).

Plumage reflects light that includes wavelengths within the visual range of birds (UV-VIS: 300–700 nm) as well as near-infrared wavelengths (NIR: 700–2,600 nm), both of which serve important roles in light and heat absorptance (Stuart-Fox et al. 2017). Within the visual spectrum, darker feathers tend to absorb more light and heat than lighter feathers (Porter and Gates 1969), but the physical properties of feathers and the ability of incident light to travel through or become captured by feather pigments and microstructures also impact the transfer of solar radiation from the sun to a bird

(Walsberg 1988; Wolf and Walsberg 2000; Stuart-Fox et al. 2018; Rogalla et al. 2022). Because NIR wavelengths are not perceived by predators, reflectance at those wavelengths is not related to camouflage, but may still play an important thermoregulatory role (Stuart-Fox et al. 2017; Medina et al. 2018).

Despite the prevalence of camouflage among animals, the majority of studies to date on background matching have focused on a small number of systems such as peppered moths (Van't Hof et al. 2011; Cook and Saccheri 2013), pocket mice (Nachman et al. 2003; Linnen et al. 2009), White Sands lizards (Rosenblum et al. 2010; Laurent et al. 2016), and a few ground-nesting birds (Troscianko et al. 2016; Stevens et al. 2017). Most camouflage systems that have been studied empirically to date involve discrete phenotypic variants that occupy visually distinct environments (e.g., tawny owls; Koskenpato et al. 2020). In comparison, continuous variation in background matching across environmental gradients has received far less attention (Stevens and Merilaita 2009; Caro et al. 2016). Furthermore, studies that simultaneously examine camouflage and thermoregulation remain scarce, especially among endotherms such as birds. Finally, the dynamics of whole-spectrum (i.e., UV-VIS-NIR) solar reflectance of epidermal surfaces and integuments in mediating relationships between camouflage and thermoregulation remains largely unexplored (but see Stuart-Fox et al. 2017; Medina et al. 2018).

To address these knowledge gaps, we examined associations between plumage reflectance and patterning, soil color and composition, and thermoregulatory models among geographically variable populations of a widespread songbird, the Horned Lark (*Eremophila alpestris*). Horned Larks occupy a variety of open habitats including

deserts, fallow agricultural land, tundra, and grasslands (Beason 1995; Mason et al. 2021; Shakya et al. 2022), where they build nests and glean seeds and insects on the ground (Wiens and Rotenberry 1979; de Zwaan and Martin 2018). Due to their preference for open habitats with sparse vegetation, larks are thought to rely on substrate matching to avoid avian predators (Donald et al. 2017). Although camouflage in Horned Larks has been discussed anecdotally (Zink and Remsen 1986; Mason and Unitt 2018), associations between phenotypic and environmental variation have not yet been quantified rigorously. Larks also exhibit various physiological adaptations to aridity gradients (Tieleman et al. 2003*b*, 2003*a*), making them an excellent system to study interactions between camouflage and thermoregulation. If larks exhibit background matching, we predict that plumage brightness, color, and patterning will be associated with variation in soil conditions to minimize visual detection. Furthermore, if plumage also plays a thermoregulatory role, we predict that birds from hotter and more arid environments will reflect more solar radiation in order to lower water requirements for evaporative cooling. Finally, if a trade-off or balance between camouflage and thermoregulation exists, we expect that there may be deviations from 'optimal' camouflage or thermoregulation phenotypes in certain environments. For example, larks in the hottest environments may have brighter than expected plumage, which would facilitate thermoregulation at the cost of less effective camouflage. Alternatively, larks in habitats where camouflage is particularly important may have solar reflectance patterns that deviate from what may be 'optimal' for thermoregulatory performance.

To test these predictions, we combined digital photography, color and plumage pattern quantification, full-spectrum (UV, Visual, NIR) spectroradiometry of museum

specimens, remote sensing data, and simulation-based thermoregulatory models of heat flux to examine phenotype-environment associations between plumage coloration and patterning, soil conditions, and climate. This approach allows us to disentangle the effects of camouflage and thermoregulation in driving the evolution and ecology of Horned Lark coloration. More broadly, it illustrates how we can understand limits on the adaptive potential of certain traits such as coloration. For example, warmer climates might select for more reflective feathers at a cost to background matching. Likewise, habitat alterations might select for darker feathers that impose greater physiological stress under warming climates. Thus, one selective pressure might have detrimental effects relative to another in the evolution of adaptive phenotypes. Only by integrating both background matching and thermoregulatory performance can we understand the evolutionary responses to these different and potentially competing selective pressures.

Methods

Digital Photography and Image Analysis

We photographed the dorsal side of 270 Horned Lark specimens from the Museum of Vertebrate Zoology (MVZ) at the University of California, Berkeley (Supplementary Table S1), using a Nikon D7000 camera modified for full-quartz calibration (Advanced Camera Services, Watton, Norfolk, England). We measured up to 10 males and 10 females of 17 different subspecies in the western United States and Mexico (Figure 1; Supplementary Figure S1), preferentially selecting specimens from breeding months (May–August) and with undamaged plumage. Individuals were assigned to subspecies in the collection based on a combination of expert opinion by

the original collector or museum curator, and by comparison with descriptions and series of the subspecies and populations in question. We note that the majority of the populations considered in this study are resident and stay largely in the same geographic region throughout their annual cycle. However, some populations are migratory and move across latitudes or altitudes during their annual cycle (Behle 1942; Beason 1995). For migratory populations, we measured specimens only from their breeding distributions.

We used a Novoflex Noflexar 30mm f/3.5 lens which does not filter out ultraviolet wavelengths and is therefore suitable for measuring plumage reflectance under an avian visual model. We took two RAW images of each specimen at ISO200: one image used a Baader Venus-U filter which captures wavelengths between ~320–380 nm, and a second image used a Baader UV/IR cut filter which captures wavelengths between ~400–680 nm. Each image included a ruler at a height equal to the top of the specimen's when photographing its dorsal side with 5% and 80% reflectance standards (Labsphere, Hutton, NH, USA). We automatically aligned and linearized images using the Image Calibration Analysis Toolbox (Troscianko and Stevens 2015) which provides a set of plugins for ImageJ (Schneider et al. 2012), and manually drew polygons corresponding to the dorsal region of each specimen in ImageJ (Supplementary Figure S2).

After processing each image and delimiting the dorsal region of interest, we converted the channel readings for the UV and visual images to the cone-catch values of a peafowl visual model, which is a "violet-sensitive" model that approximates the spectral sensitivities of foraging raptors (Martin and Osorio 2008; Lind et al. 2013). We

selected this model because raptors such as falcons and hawks are the most likely predator of Horned Larks and the potential receiver against which larks are trying to avoid visual detection (Smith and Murphy 1973; Marti and Braun 1975). We then converted these cone-catch values into tetracolorspace measurements (Vorobyev et al. 1998; *sensu* Stoddard and Prum 2008) of hue and achieved chroma using the package pavo v2.2.0 (Maia et al. 2013, 2019) in the R programming environment (R Core Team 2021). Hue includes two angular measurements, theta and phi, which together describe the location of the plumage patch in tetracolorspace. Achieved chroma (also referred to as saturation) is the distance of a plumage patch from the achromatic center in tetracolorspace. We also measured achromatic brightness (i.e., total reflectance or luminosity across all wavelengths) and calculated an index of patterning via Fast Fourier Transform (FFT) bandpass filters at 49 levels (beginning at 2 pixels and increasing exponentially by $\sqrt[8]{2}$ to 128). FFTs are widely applied in digital image analysis (Stoddard and Osorio 2019) and can be used to quantify animal patterns based on neurophysiological processing of spatial patterns (Godfrey et al. 1987; Stoddard and Stevens 2010; Troscianko et al. 2016; Mason and Bowie 2020). In this process, an image is converted into a set of sine waves that each have a different frequency and amplitude. The amplitude or power of each wave indicates how much patterning, i.e., change between light and dark pixels, occurs at a specific spatial scale. Thus, images with high power across FFT bandwidths display more patterning (e.g. the dorsal spots on some larks), whereas images with lower power are more uniformly colored.

Summing these values across frequencies provides a measure of "total power" for the plumage pattern.

We also performed a principal component analysis on all of the coloration metrics—brightness, hue (theta and phi), achieved chroma, and dorsal patterning (total power)—to summarize plumage variation among the sampled larks. We found that the first principal component axis loaded positively with brightness and achieved chroma, whereas the second principal component axis loaded positively with brightness and patterning but negatively with redness (Supplementary Table S2).

Measuring Full-spectrum Solar Reflectance

We measured solar reflectance of the Horned Lark specimens described above using recently published methods for estimating heat stress in birds (Riddell et al. 2019). For each specimen, we measured dorsal and ventral feather reflectance from 350 – 2500 nm using an ASD FieldSpec Pro spectroradiometer (ASD, Inc., 1625 S. Fordam Street, Suite 300, Longmont, CO 80503), and standardized each measurement relative to a Spectralon™ white standard before recording our measurements. We used a custom-built tungsten halogen light source to measure feather reflectance 2 cm from the feather surface, with a 45° angle between the light source and fiber optic cable. This light source was built using an AC-to-DC voltage converter to inhibit interference from an alternating source of electrical current. To standardize the angle and distance, we used a RPH-1 reflection probe holder (Ocean Optics, Inc., Largo, FL). We also used the reflection probe to standardize the surface area of each measurement. The combination of ten measurements per specimen (see below) and the diameter of the probe opening

(6.35 mm) ensured that we captured the average solar reflectance of the dorsal and ventral side for each specimen.

We used ViewSpec software (ASD, Inc.) to measure solar reflectance by recording ten measurements (five dorsal and five ventral) for each of the 270 specimens. On both the dorsal and the ventral sides, we recorded one measurement from the crown or neck and four measurements spread across the breast or mantle for a total of 2,700 measurements. We then used a custom script in Python (v. 3.5; https://github.com/mason-lab/HornedLarkCamoThermo) to average these values for each individual, and corrected the reflectance curves for solar radiation using the ASTM G-172 standard irradiance spectrum for dry air provided by SMARTs v. 2.9 (Gueymard 2001). We calculated the corrected value by multiplying the intensity of solar radiation by the empirical reflectance, integrating across all of the wavelengths, and dividing by the total intensity of solar radiation (Gates 1980).

Environmental Data

We compiled two different soil data sets to examine associations between Horned Lark dorsal plumage and soil conditions. First, we downloaded a soil color data set based on an extensive series of United States Department of Agriculture soil surveys of the contiguous United States, with values that had been converted from Munsell color charts to RGB color space at a resolution of 200 m (Beaudette et al. 2013). We extracted soil condition data corresponding to georeferenced localities of each lark specimen obtained from the MVZ database Arctos (arctos.database.museum). To account for uncertainty in the reported coordinates of

georeferenced localities for the vouchered specimens (average = 8.9 km ± 17.6 km SD), we extracted values for 50 points randomly generated within a 5 km radius of each coordinate. We then took the average of those 50 samples for each vouchered specimen and each raster for downstream analyses. Next, we extracted their respective soil values and performed a principal components analysis to include in downstream analyses of soil color. The first principal component axis loaded strongly with all three channels corresponding to soil brightness. The second principal component axis loaded positively with the red channel, but negatively with blue and green (Supplementary Table S3), and therefore corresponded to soil redness. In this manner, we obtained soil color data associated with the site of collection for 224 of our Horned Lark specimens. Because this soil color dataset is limited to the continental United States, we were unable to include 46 individuals from populations in Alaska, Canada, and Mexico in this part of our study.

We also downloaded harmonized soil property data for the top five centimeters of soil depth at a 30 arc-second resolution (approximately 1 km) from the WISE30Sec database (Batjes 2016). WISE30Sec data have been used widely to study soil biogeochemistry for quantifying global carbon stocks (Sanderman et al. 2017). Although this dataset has not been applied broadly to organismal biology, it provides ecologically relevant information on clay abundance, proportion of coarse fragments, and other soil properties relevant to terrestrial organisms such as Horned Larks, which prefer open areas with little to no vegetation (Wiens et al. 1987). To generate an index of soil surface granularity, we extracted the volume percentage of coarse fragments (> 2 mm) and the mass percentages of sand, silt, and clay. We then performed a principal

component analysis for use in subsequent analyses and found that the first principal component axis loaded positively with coarse fragments and sand, and negatively with silt and clay (Supplementary Table S4).

To examine associations between climate and plumage, we also downloaded all 19 WorldClim bioclimatic variables (worldclim.org; Hijmans et al. 2005) at a resolution of 30 arc-seconds (approximately 1 km) to examine associations with dorsal plumage and to construct models of cooling costs. We conducted a principal component analysis for downstream analyses in which the first principal component axis loaded positively with seasonality, the second principal component axis loaded positively with aridity, and the third principal component axis loaded positively with temperature (Supplementary Table S5).

Statistical Analyses of Phenotype-Environment Associations

We performed a series of statistical analyses to examine associations between dorsal plumage and the environment. First, we summarized phenotypic variation among subspecies by plotting the first two PCA axes of plumage variation and noted clustering by subspecies and sex. We then compared mean values by first performing an analysis of variance on the output of linear models, with subspecies as the grouping variable and with males and females separately. We subsequently used a Tukey's multiple comparison post-hoc test (Steel et al. 1997) with the HSD test function from the agricolae package v1.3-3 (de Mendiburu 2020) in R (v4.1.1; R Core Team 2021) to assign subspecies to groups within each sex based on their mean values and also look for differences between males and females across subspecies.

We constructed linear models (LMs) in R (v4.1.1; R Core Team 2021) to quantify phenotype-environment associations between plumage metrics and multiple main effects including soil brightness (soil color PC1), soil redness (soil color PC2), soil granularity (soil granularity PC1), aridity (bioclim PC2), temperature (bioclim PC3), sex, and specimen age. Horned Larks in the western United States exhibit little to no phylogeographic structure among most subspecies and populations (Mason et al. 2014); thus, we did not include any covariate of relatedness in our statistical analyses. We included sex because coloration and patterning can vary between male and female Horned Larks (Beason 1995). We also included specimen age because our specimens were collected over a large time span (1875–2002) and colors of specimens sometimes change as years pass since their initial collection (Armenta et al. 2008; Doucet and Hill 2009). We examined collinearity among our predictor variables by calculating correlation coefficients among each pair of main effects. The five plumage metrics that we examined as response variables in our LMs included plumage brightness, achieved chroma, hue (theta), hue (phi), and dorsal patterning (power).

Heat flux simulations

We incorporated empirical measurements of solar-corrected feather reflectance into a heat flux model to estimate the thermoregulatory differences among larks across environmental conditions in the western United States. This model simulates heat balance using the morphological characteristics of each bird in a complex radiative and thermal environment. The simulation output produces estimates of net sensible heat flux (Q), which was calculated using:

$$Q = M - E - C\frac{dT_b}{dt} = K_e(T_b - T_e) \quad \text{Eq.1}$$

where *M* is the heat generated through metabolic processes, *E* is the heat lost via evaporative processes, C is the capacitance of the isothermal core, T_b is body temperature, K_e is the effective conductance, and T_e is the operative temperature. The net sensible heat flux equation estimates the heat flux required to maintain a stable body temperature given the morphology of the bird and its interaction with the environment.

The heat flux simulation uses biophysical principles to estimate heat flux between the birds and their environment. We used environmental data generated by *NicheMapR* (v1.1.3; Kearney and Porter 2020) to estimate the thermal microclimate for Horned Larks. First, we obtained monthly minimum and maximum air temperatures from the *Worldclim* global climate database for the sites at which specimens had been collected (Fick and Hijmans 2017). We then corrected these temperatures using *NicheMapR* to reflect conditions relevant to larks, using a reference height of 5 cm above the ground because larks spend most of their time near the ground. We simulated heat flux assuming two types of soil environments: a xeric, desert-like environment (sand, soil reflectance = 0.35) and a more mesic environment (loam, soil reflectance = 0.15; Campbell and Norman 1998). These two environments represent the extremes of the thermal environment that Horned Larks inhabit in our study area. Assuming a more reflective soil (i.e., sand) in our simulations did not qualitatively alter our conclusions; therefore, we present our analyses assuming the loam soil. We then used these environments to assess the thermal consequences of variation in dorsal solar-corrected feather reflectance.

We incorporated morphological phenotypes that directly influence reflected solar radiation in several ways. Our goal was to isolate the importance of dorsal reflectance for thermoregulation. Thus, we assumed that each phenotype was equivalent among subspecies, with the exception of feather reflectance. In general, variation in recorded body mass among the specimens we examined was low (64 males = 30.2 g ± 3.65 standard deviation, 70 females = 28.61 g ± 3.66), suggesting that the differences in mass were unlikely to substantially influence thermoregulatory differences among subspecies. Thus, we used a mean body mass (29.5 g) for all subspecies in our simulations. This value was determined by Riddell et al. (2019) by searching for body mass measurements of Horned Larks in western North American using the Vertnet data aggregator (vertnet.org, n = 2,468). The protocol in Riddell *et al*. (2019) removed data greater or less than two standard deviations from the mean body mass to remove values from juvenile birds erroneously labelled as adults and extreme outliers that likely reflect an error in measurement . Estimates of mass agree closely with previously published values for subspecies of Horned Larks (Behle 1942). Estimates of feather phenotypes were taken from Riddell et al. (2019) using three specimens that represented the average mass of a Horned Lark in our simulations, but here we briefly describe our methodology. We estimated plumage depth (sensu Kearney et al. 2016) by measuring the vertical distance from the skin to the outer surface of the feathers using a Fisherbrand™ 150 mm ruler at 10 locations that spanned the dorsal and ventral side of each specimen. We also measured the average length of contour feathers across six feathers per specimen spanning the dorsum and ventrum. To characterize the approximate shape of Horned Larks, we used measurements of the height, length, and

width of each specimen. We measured length from the crown to vent, width from shoulder to shoulder, and height from the back of the dorsal side to the breast at the shoulder (Kearney et al. 2019). We then used these values to estimate the rough dimensions of a Horned Lark, assuming a spheroid shape (Porter and Kearney 2009). The dimensions of birds in nature are dependent upon posture and thus are highly variable. By using the same dimensions for each subspecies, our analysis focuses on the thermoregulatory effects of reflectance and avoids possible noise due to specimen preparation and behavioral differences among subspecies.

The simulations estimate heat flux by integrating morphological phenotypes with environmental biophysics and behavior. Estimating heat flux in endotherms is complicated by properties of the insulation layer. We addressed these issues by integrating a series of equations involved in a two-dimensional heat transfer model to estimate the flux from the dorsal and ventral components of a bird (Bakken 1981). This model calculates the total amount of heat absorbed or lost from the environment and converts the amount of energy into the physiological response that would be necessary to maintain a stable body temperature (39ºC in our simulations). These values represent the amount of heat that needs to be generated via metabolic heat production or lost via evaporative cooling to regulate body temperature. We incorporated different sources of heat, including air temperature, direct solar radiation, diffuse solar radiation, reflected radiation from the ground and sky, and longwave radiation from the sky and ground. For our simulations, we assumed a windspeed of 0.1 m/s, which likely reflects near ground convective conditions (Gates 1980). The specific calculations for these simulations can

be found in Riddell *et al*. (2019) and the Python script can be found on GitHub (https://github.com/ecophysiology/Endoscape).

We used these simulations to isolate the thermoregulatory consequences of geographic variation in dorsal feather absorptance, where absorptance is the reciprocal of reflectance. We were specifically interested in estimating the water requirements for evaporative cooling (termed 'cooling costs') because these costs are highly relevant to the environmental pressures shaping physiological adaptation in Horned Larks (Tieleman et al. 2003*a*). We estimated cooling costs across all sites with available climate and elevational data (n = 70). For all sites, we generated estimates of cooling costs using two simulations: one with the solar-corrected average dorsal absorptance across all sites (average = 0.74) and the other incorporating the solar-corrected, site-specific dorsal absorptance (range = 0.65 – 0.80). Ventral feather absorptance was held constant (average across all specimens = 0.60) to specifically focus on the role of dorsal feather absorptance in camouflage and thermoregulation. For each site, we subtracted the cooling costs between the two simulations. The difference (termed 'cooling benefit') provides an index for the site-specific reduction in thermoregulatory pressure driven by geographic variation in dorsal feather absorptance, where positive values indicate lower costs than average and negative values indicate higher costs than average.

We then fit exponential models from the *nls*() function in *R* (v4.0.1; R Core Team 2021) to determine the relationship between the cooling benefits and the principal components of climatic variables. For climatic variables, we used the site-specific values that described seasonality (PC1), aridity (PC2), and temperature (PC3; see Supplementary Table S6 for loadings). Starting values for coefficients were generated

using the *nlsLM*() function. We assessed the significance of the models based on the regression coefficients and 95% confidence intervals. We generated 95% confidence intervals with a bootstrapping method using 1,000 samples with the *replicate*() function in *R*. We then used an AIC model selection framework to determine whether models with the principal components of seasonality, aridity, or temperature were more likely to explain the variation in the reduction in cooling costs attributed to variation in feather absorptance.

Statistical Analyses of a Trade-off Between Camouflage and Thermoregulation

To test for a trade-off between camouflage and thermoregulation, we first extracted residual values from our full linear model with plumage brightness as a response variable and soil brightness, soil redness, soil granularity, sex, and years since collection as main effect predictor variables. Positive or negative residual values indicate individuals that are brighter or darker than expected based on environmental conditions. We then compared these values to cooling benefits for each individual, which were calculated using a similar method as the cooling benefits analysis above but from the perspective of individuals rather than sites. We ran two simulations: one in which we generated values for cooling costs for individuals at their collection location using the observed individual variation in solar-corrected absorptance, and another in which we used the average solar-corrected dorsal absorptance. We then calculated the difference in cooling costs between simulations with average and observed dorsal absorptance to generate an individual-level cooling benefit. We restricted the analysis to 203 specimens from sites with microclimatic data available (the remaining 67

specimens were from sites without these data). Higher values correspond to individuals that experienced higher cooling benefits than an individual with average absorptance, whereas lower values indicate individuals that experience higher thermoregulatory costs than an average individual. We then built a linear model with residual brightness as a response variable and cooling benefits as a predictor variable to test for a tradeoff between camouflage and thermoregulation.

Results

Phenotypic variation

Plumage characters varied among subspecies and sexes but also exhibited substantial overlap, as illustrated by the PCA of plumage characters (Figure 2A; see Supplementary Figure S3 for convex hull polygons of subspecies and sex groupings). For example, *E. a. leucansiptila* of the Colorado Desert tended to have higher PC1 and PC2 scores, indicating that they were lighter and had more dorsal patterning compared to other subspecies. In parallel with PCA scores and loadings, we found that *E. a. leucansiptila* was in its own posthoc group for brightness for both males (Figure 2B) and females (Figure 2C). In contrast, *E. a. rubea* tended to be darker, more saturated, and more red than other subspecies. Further comparisons of mean values using Tukey's posthoc tests revealed various groupings among both male and female Horned Larks, but also indicated substantial overlap or gradations in phenotypes among subspecies (Figure 2B–K; Supplementary Figures S4–S13). Geographically proximate subspecies often had overlapping plumage measurements. For example, the geographic distribution of *E. a. ammophila* overlaps with *E. a. actia* to the west in south-central

California, and the two subspecies exhibited substantial overlap in posthoc groupings. Similar overlap was present in other pairs of geographically proximate subspecies such as *E. a. occidentalis* and *E. a. adusta*, which come into contact in southern Arizona. Overall, these results suggest substantial geographic variation in plumage coloration and patterning among Horned larks across the western United States, but also suggest clinal change among many adjacent populations, as noted elsewhere (Behle 1942).

We also uncovered differences in mean values between males and females across all subspecies (Supplementary Figure S14). Specifically, females had higher hue (theta) and dorsal patterning (power) values on average, while males had higher hue (phi) values on average.

Phenotype-environment associations

Using linear models, we found multiple associations between dorsal plumage variation and soil conditions, climatic variables, sexual dimorphism, and years since collection (Figure 3; Table 1). These results support long-held postulates that Horned Larks exhibit strong phenotype-environment associations in coloration and patterning (Behle 1942). Specifically, we found that dorsal brightness was positively associated with soil granularity (Fig. 3C), aridity (Fig. 3D), and temperature (Fig. 3E), while achieved chroma (saturation) was positively associated with soil redness (Fig. 3F) and temperature (Fig. 3J; Table 1). Hue (theta) was negatively associated with soil redness (Fig. 3L), soil granularity (Fig. 3M), aridity (Fig. 3N), temperature (Fig. 3O), sex_{male} (Supplementary Figure S14), and years since collection (Supplementary Figure S15). The second component of hue (phi) was positively associated with soil redness, $sex_{male,}$

and years since collection but was negatively associated with soil granularity (Table 1). Finally, dorsal patterning was positively associated with soil granularity and negatively associated with sex_{male} (Table 1).

The predictor variables included in our linear model were largely uncorrelated with each other (Supplementary Figure S16), but the strongest correlations were a positive correlation between soil brightness and soil granularity ($r^2 = 0.55$) and between soil brightness and aridity ($r^2 = 0.53$). All other pairwise correlations were below $r^2 < 0.50$.

Heat Flux Simulations

The observed variation in feather absorptance improved cooling benefits compared to simulations with average feather absorptance. Of the 70 sites with available climate and elevational data, simulations with the observed variation in absorptance exhibited lower cooling costs relative to simulations with average absorptance for 31 sites (44.3%), higher cooling costs for 25 sites (35.7%), or did not change (14 sites, 20%). For sites that benefitted from the reductions in feather absorptance, cooling costs declined by 13.9% on average (range = 0.7% to 60.7%). The cooling benefits were also positively associated with temperature (PC2) and aridity (PC3) indices but not with seasonality (PC1; Figure 4, Supplementary Table S6). Although the reduction in cooling costs was associated with both temperature and aridity (Table 2), model selection indicated that the model with aridity outperformed models with temperature and seasonality (Supplementary Table S6).

Testing for a Trade-off Between Camouflage and Thermoregulation

We found that residuals of plumage brightness taken from our linear model—with soil brightness, soil redness, soil granularity, aridity, temperature, sex, and specimen age as main effects—was positively correlated with individual estimates of cooling benefits based on our thermoregulatory models ($\boldsymbol{\beta}_{\text{Cooling cost}} = 0.035 \pm 0.011$; T-value = 3.35; P-value = 9.96 e-4; Figure 5). In other words, some individuals were brighter than would be expected based on environmental conditions, and those individuals also had higher cooling benefits based on the solar absorptance of their plumage. Conversely, some individuals were darker than would be expected based on environmental conditions and had reduced cooling benefits.

Discussion

By combining data from digital photography, spectroradiometery, thermal modeling, and remote sensing we documented multiple associations between dorsal plumage and environmental conditions of Horned Larks over a broad geographic distribution. These findings emphasize the multifarious role of feathers and animal coloration more generally. Although lark coloration has long been hypothesized to facilitate camouflage (Behle 1942; Donald et al. 2017; Mason and Unitt 2018), our study provides the first empirical evidence of phenotype-environment associations that underlie background matching in Horned Larks in brightness, hue, and patterning. The associations between color and climate that we uncovered largely followed Gloger's Rule, although we found some slight differences from predicted trends. Furthermore, full-spectrum spectroradiometry combined with simulation-based models of

thermoregulation revealed that geographic variation in feather reflectance reduces evaporative cooling costs in hotter and drier environments. While selective pressures imposed on total solar reflectance in feathers have just begun to be explored (Stuart-Fox et al. 2017; Medina et al. 2018), our findings suggest that the interaction between feathers and the full spectrum of sunlight (UV-Vis-NIR) play an important role in the thermal ecology of Horned Larks. Here, we discuss our findings in the context of each of these ideas in more detail.

Background Matching

Background matching by resembling a random sample of the substrate is one component of a suite of phenotypes that organisms have evolved to avoid visual detection by predators (Merilaita and Lind 2005; Stevens and Merilaita 2009). We found various plumage-substrate associations underlying background matching in Horned Larks. The strongest association we found between plumage brightness and soil conditions was a positive association with soil granularity (Table 1; Fig. 3C), while we did not find an association between plumage brightness and soil brightness in our full linear models (Table 1; Fig. 3A). Rather than a direct, adaptive association between plumage brightness and soil granularity, we suspect that these statistical patterns reflect substantial collinearity between soil brightness and other environmental conditions (Supplementary Fig. S16). In fact, linear models that include soil brightness as the sole predictor of plumage brightness revealed a strong association between the two variables ($\boldsymbol{\beta}_{\text{Soil PC1}}$ = 7.48 e-04 ± 6.10 e-05; P = 8.82 e-27). We also found strong associations between plumage 'redness'—both in terms of chroma or saturation and

hue—and soil redness (Table 1; Fig. 3G; Fig. 3L; Fig. 3Q) in our full linear models. Thus, in general, we found that variation in dorsal brightness and hue in Horned Larks matched background substrates, as has been shown in mice (Vignieri et al. 2010), gerbils (Boratyński et al. 2017), moths (Kettlewell 1955), and other taxa (Stevens et al. 2014; Troscianko et al. 2016). To our knowledge, our study is the first to quantify both animal and substrate color to provide rigorous evidence in support of geographic variation in camouflage on a continental scale.

Background matching in Horned Larks also involves dorsal patterning, in which increased dorsal 'mottling' with more high-contrast spots was associated with increases in sand and other coarse particles rather than with clay and silt (Fig. 3W). There is less empirical evidence for background matching in pattern as opposed to brightness or color alone, but it has been reported in cuttlefish (Barbosa et al. 2008), nightjars (Troscianko et al. 2016), and plover eggs (Stevens et al. 2017). Beyond background matching, increased dorsal patterning in Horned Larks also may contribute to disruptive patterning that breaks up the visual outline of the bird as seen by predators from above (Cuthill et al. 2005). Disruptive patterning in larks may be associated with molt strategies that promote the retention of worn feathers with lighter edges that further obscure individuals from visual detection (Negro et al. 2019).

Plumage-Climate Associations: Unpacking Gloger's Rule

We uncovered strong associations between dorsal plumage and climate. In fact, the strongest association we found across all of our linear models was between dorsal brightness and aridity (Table 1; Fig 3D), while dorsal brightness was also strongly

associated with temperature (Table 1; Fig 3E). These findings correspond with the predictions of the "simple" version of Gloger's Rule, such that lighter-colored larks with less melanin overall (i.e., eumelanin and pheomelanin combined) were found in hotter, more arid environments (Gaston et al. 2008). We also found that plumage saturation or chroma was positively associated with temperature (Table 1; Fig 3J), while redness (hue (theta)) was associated with both aridity (Table 1; Fig. 3N) and temperature (Table 1; Fig. 3O). These latter findings correspond to the 'complex' version of Gloger's Rule, which predicts more rufous or redder coloration produced by pheomelanin in hotter, more arid environments (Delhey 2019).

An emerging discussion in the literature involves unpacking Gloger's Rule to better understand the biological phenomena driving widespread ecogeographic patterns in melanism (Delhey et al. 2019; Caro and Koneru 2021). For example, a recent study found that light environments can play an important role in shaping associations between coloration and climate (Marcondes et al. 2021). Horned larks exist across a wide variety of environments that differ in soil and climate conditions, but they are all "open" habitats with little to no vegetation or structure, suggesting that light environments play a negligible role in shaping lark coloration. In the case of our linear models of lark dorsal brightness, which corresponds to the total amount of melanin (eumelanin and pheomelanin combined), climate had a stronger association than soil conditions overall. However, soil color, soil composition, and climate are inextricably linked: organic matter, mineral content, microorganisms, water, and air all interact to produce soil color via pedogenesis, which are in turn related to temperature, humidity, and seasonality (Owens and Rutledge 2005). This interdependency makes determining

the relative impacts of soil conditions (i.e., background matching) and climate (i.e., thermoregulation) on lark plumage melanin content and coloration difficult to disentangle. Our study suggests that both background matching via soil conditions and thermoregulation via climate contribute to the ecogeographic patterns observed in Horned Lark coloration as well as similar patterns in other taxa (Delhey 2019).

Thermoregulatory Models

Our thermoregulatory models found that cooling benefits estimated from full-spectrum solar absorptances were associated with temperature (Fig. 4B) and aridity (Fig. 4C). Interestingly, cooling benefits increased in a non-linear fashion and were substantially higher on average at localities with extremely high temperatures and aridity—presumably to prevent Horned Larks from overheating and becoming dehydrated. Our modeling approach for estimating cooling benefits incorporates numerous parameters such as direct and diffuse solar radiation, feather conductance, and radiation reflected from the ground (Gates 1980). Solar radiation includes both reflected light that is readily perceived by birds (300–700 nm; UV-VIS wavelengths) and near-infrared radiation (700-2100 nm) that is to invisible to vertebrates yet could play an important role in thermoregulation (Clusella Trullas et al. 2007; Stuart-Fox et al. 2017; Medina et al. 2018). NIR reflectance can differ considerably among coloration mechanisms (Shawkey et al. 2017), yet the extent to which NIR reflectance can vary independently from UV-VIS reflectance within and among different coloration mechanisms is not fully known. However, a recent study demonstrated pronounced differences in NIR reflectance among different white plumage patches of birds that

correspond to differences in feather barb morphology and density (Stuart-Fox et al. 2018). This suggests that feather microstructure could play an important role in shaping reflectance at different wavelengths across the spectrum of solar radiation, with implications for how phenotypes balance competing pressures for camouflage and thermoregulation.

There are many other factors beyond modifications to solar reflectance in UV-VIS and NIR wavelengths that could contribute to the ability of Horned Larks to inhabit hot, arid environments (Trost 1972; Dean and Williams 2004). First, many arid-adapted larks have reduced metabolic rates and increased water retention through various physiological adaptations (Tieleman et al. 2002). Therefore, our study adds further support to the importance of conserving water in hot and arid environments. Second, behavioral adaptations also can reduce heat stress. For example, microhabitat selection such as resting in shade or animal burrows during extreme heat may contribute to thermoregulation in larks (Williams et al. 1999; Hartman and Oring 2003; Walde et al. 2009). While Horned Larks are philopatric and stay close to their breeding territory during the breeding season (Beason 1970), they are generally nomadic during non-breeding months and may seek out favorable habitat within reach of their individual movements to facilitate thermoregulation. Feather coloration and reflectance is one part of a complex suite of phenotypes involved in maintaining homeostasis in thermally challenging environments. The interplay of plumage and other physiological and behavioral adaptations for thermoregulation remains an open and exciting avenue of future research.

Balancing Camouflage and Thermoregulation

In addition to uncovering a general trend of background matching between Horned Larks and the substrate on which they exist, we identified certain individuals that had high residual plumage brightness—suggesting that they were either much lighter or darker than expected based on the environmental predictors included in our models. These residual values were associated with cooling costs (Fig. 5), such that deviations from an 'optimal' plumage brightness may be related to thermoregulatory pressures. This trend is illustrated by two subspecies on either extreme of our data set: *E. a. rubea*, which was darker than expected and occurs in the Sacramento Valley; and *E. a. leucansiptila*, which was lighter than expected and occurs in the Colorado Desert.

These two populations differ in aspects of their life history that may explain in part the trade-off between camouflage and thermoregulation. Horned Larks of the dark, red subspecies *E. a. rubea* (Fig. 2) are resident in the hot Sacramento Valley, which has very clay-rich soil of a ruddy hue that is restricted geographically and is quite different from nearby soil conditions. As permanent residents, *E. a. rubea* may have as many as three broods per year (Behle 1942) and therefore spend more time breeding and caring for young compared to high-latitude, migratory populations of Horned Larks that only have sufficient time for a single brood (Verbeek 1967). We speculate that the highly localized soil conditions combined with the extended breeding season of larks in the Sacramento Valley may have promoted the evolution of darker, redder plumage than might otherwise be expected based on environmental conditions alone. In this instance, camouflage may have evolved to promote survival during a prolonged breeding season at the expense of thermoregulation in a hot environment. At the other extreme, *E. a.*

leucansiptila is the palest of the lark subspecies we measured (Fig. 2) and is resident in the hottest and most arid region included in our study: the Colorado Desert. The soil composition of the Colorado Desert is variable and includes alluvial deposits from the Colorado River, sand hills, salt flats, dry lake basins, and agricultural land. The exact number of broods and the corresponding length of the breeding season for *E. a. leucansiptila* is unknown, but we speculate that larks in the Colorado Desert are lighter than might be expected because of the extremely hot and arid weather conditions and the heterogeneity of the soil.

Taken together, these examples suggest a trade-off between plumage and camouflage that is perhaps dictated by the degree and variation in environmental conditions combined with differences in life history traits. Similar phenomena may drive differences in coloration among other populations and species as well.

Temporal Considerations

Our study quantified associations between various contemporary environmental data sets and Horned Lark coloration phenotypes from museum specimens, the latter of which were collected across a large time span (1875–2002). We included older specimens for some populations and subspecies because of the limited sampling in certain regions. Thus, there is a potential temporal mismatch between the specimen data and the environmental conditions against which camouflage and thermoregulation are being quantified. Furthermore, there is evidence that Horned Lark plumage has shifted over contemporary time scales in response to rapid habitat change in certain populations (Mason and Unitt 2018). However, the goal of our study was to quantify

phenotype-environment associations over broad, evolutionary time scales that may have given rise to local adaptation in background matching among lark populations over many thousands or millions of years. As such, the phenotypic and environmental data sets were collected at roughly similar time points on an evolutionary time scale of many millennia. That said, Horned Larks are an excellent system for studying how populations respond to anthropogenic change such as agriculture or climate (Mason and Unitt 2018; Mason et al. 2021), and continued scientific collecting may provide opportunities to study how phenotype-environment associations may change in the in the future.

Our phenotype-environment associations were generated from localities where the specimens were collected, thus representing a snapshot in the annual cycle of Horned Larks. Most lark populations are largely resident, but some populations that breed at higher latitudes or elevations are migrants that must thermoregulate and avoid visual detection in multiple environments and substrates that differ in color and composition. Adding to the complexity of this challenge, soil color may change over the course of a year as precipitation increases or decreases, especially in more seasonal environments. Adult Horned Larks molt only once per year (Pyle 1997), and thus migratory populations may need to balance competing pressures for background matching and thermoregulation in different environmental conditions with the constraint of a single, year-round plumage. Future studies could expand on our results by examining how natural selection balances potentially competing pressures—like camouflage and thermoregulation—across dynamic annual cycles involving movement and seasonal change.

Conclusion

Our study uncovered empirical evidence for the multifaceted role that plumage plays in mediating both camouflage and thermoregulation in Horned Larks. Dorsal plumage coloration and patterning are associated with soil conditions and climate, while solar reflectance of plumage confers cooling benefits in hot and arid environments. We also observed evidence of a potential tradeoff between camouflage and thermoregulation. Future studies could leverage these phenotype-environment associations in combination with genomic resources (e.g., Mason et al. 2020) to identify candidate loci driving these local adaptations. Furthermore, Horned Larks are one of approximately 100 species of larks (Alaudidae) globally that vary in plumage and habitat affiliations. Many other lark species exhibit similarly extensive geographic variation in coloration and presumably background matching, including interesting examples of both clinal and more discrete differences in plumage and habitat affinities (Donald et al. 2017). Phylogenetic comparative studies across the family would shed light on whether the patterns we found here are generalizable across broader taxonomic and evolutionary scales. Interactions between an organisms' body surfaces and light from the sun are complex, and our study illustrates how natural selection has shaped the phenotypic variation across different habitats to meet potentially competing demands.

Acknowledgements

We are grateful to Emma Arulanantham for their help in photographing larks. Russel Ligon and Jolyon Troscianko provided guidance in developing the digital photography setup and photo processing pipeline. We thank Nick Horrocks, an anonymous peer

reviewer, and editors Daniel Bolnick, Sean O'Donnell, and Bob Montgomery for their constructive input while revising our manuscript. The late Ned K. Johnson collected many of the lark specimens used in this study. N.A.M. was supported by an NSF Doctoral Dissertation Improvement Grant (DEB-1601072) and an NSF Postdoctoral Biology Fellowship (DBI-1710739). E.A.R. was supported with funding from an NSF Grant (DEB-1457742).

Statement of Authorship

N.A.M., C.C., and R.C.K.B. conceived the study; N.A.M., E.A.R., and F.G.R. collected the data; N.A.M. and E.A.R. analyzed and visualized the data; C.C. collected and provided access to specimens used in the study; C.C. and R.C.K.B. supervised the project; N.A.M. wrote the first draft of the manuscript with subsequent edits by E.A.R., F.G.R., C.C. and R.C.K.B.

Data and Code Availability

Raw data, metadata, and annotated code to reproduce the analyses and figures presented in this manuscript are available via Dryad (https://doi.org/10.6078/D1ZX4S; Mason et al. 2022).

Literature Cited

Andersson, M., and L. W. Simmons. 2006. Sexual selection and mate choice. Trends in Ecology & Evolution 21:296–302.

Armenta, J. K., P. O. Dunn, and L. A. Whittingham. 2008. Effects of specimen age on plumage color. The Auk 125:803–808.

Bakken, G. S. 1981. A two-dimensional operative-temperature model for thermal energy management by animals. Journal of Thermal Biology 6:23–30.

Barbosa, A., L. M. Mäthger, K. C. Buresch, J. Kelly, C. Chubb, C.-C. Chiao, and R. T. Hanlon. 2008. Cuttlefish camouflage: The effects of substrate contrast and size in evoking uniform, mottle or disruptive body patterns. Vision Research 48:1242–1253.

Batjes, N. H. 2016. Harmonized soil property values for broad-scale modelling (WISE30sec) with estimates of global soil carbon stocks. Geoderma 269:61–68.

Beason, R. 1970. *The annual cycle of the Prairie Horned Lark in west-central Illinois* (Master's Thesis). Western Illinois University, Macomb.

Beason, R. C. 1995. Horned Lark (Eremophila alpestris), version 2.0. In The Birds of North America (A. F. Poole and F. B. Gill, Editors). Cornell Lab of Ornithology, Ithaca, NY, USA.

Beaudette, D. E., P. Roudier, and A. T. O'Geen. 2013. Algorithms for quantitative pedology: A toolkit for soil scientists. Computers & Geosciences 52:258–268.

Behle, W. 1942. Distribution and variation of the horned larks (*Eremophila alpestris*) of western North America. University of California Publications in Zoology 46:203–316.

Boratyński, Z., J. C. Brito, J. C. Campos, J. L. Cunha, L. Granjon, T. Mappes, A. Ndiaye, et al. 2017. Repeated evolution of camouflage in speciose desert rodents. Scientific Reports 7:1–10.

Burtt, E. H. 1981. The adaptiveness of animal colors. BioScience 31:723–729.

———. 2004. Gloger's Rule, feather-degrading bacteria, and color variation among song sparrows. Condor 106:681–686.

Campbell, G., and J. Norman. 1998. An introduction to environmental biophysics (2nd edition.). Springer-Verlag, New York, NY.

Caro, T. 2017. Wallace on Coloration: Contemporary Perspective and Unresolved Insights. Trends in Ecology & Evolution 32:23–30.

Caro, T., K. Brockelsby, A. Ferrari, M. Koneru, K. Ono, E. Touche, and T. Stankowich. 2021. The evolution of primate coloration revisited. (L. Simmons, ed.)Behavioral Ecology 32:555–567.

Caro, T., and M. Koneru. 2021. Towards an ecology of protective coloration. Biological Reviews 96:611–641.

Caro, T., T. N. Sherratt, and M. Stevens. 2016. The ecology of multiple colour defences. Evolutionary Ecology 30:797–809.

Clusella Trullas, S., J. H. van Wyk, and J. R. Spotila. 2007. Thermal melanism in ectotherms. Journal of Thermal Biology 32:235–245.

Cook, L. M., and I. J. Saccheri. 2013. The peppered moth and industrial melanism: Evolution of a natural selection case study. Heredity 110:207–212.

Cott, H. B. 1944. Adaptive Coloration in Animals. Bradford and Dickens Drayton House, London.

Cuthill, I. C., W. L. Allen, K. Arbuckle, B. Caspers, G. Chaplin, M. E. Hauber, G. E. Hill, et al. 2017. The biology of color. Science 357:eaan0221.

Cuthill, I. C., M. Stevens, J. Sheppard, T. Maddocks, C. A. Párraga, and T. S. Troscianko. 2005. Disruptive coloration and background pattern matching. Nature 434:72–74.

de Mendiburu, F. 2020. agricolae: Statistical Procedures for Agricultural Research.

de Zwaan, D. R., and K. Martin. 2018. Substrate and structure of ground nests have fitness consequences for an alpine songbird. Ibis 160:790–804.

Dean, W. R. J., and J. B. Williams. 2004. Adaptations of birds for life in deserts with particular reference to Larks (Alaudidae). Transactions of the Royal Society of South Africa 59:79–91.

Delhey, K. 2019. A review of Gloger's rule, an ecogeographical rule of colour: definitions, interpretations and evidence. Biological Reviews brv.12503.

Delhey, K., J. Dale, M. Valcu, and B. Kempenaers. 2019. Reconciling ecogeographical rules: rainfall and temperature predict global colour variation in the largest bird radiation. Ecology Letters 22:726–736.

Donald, P. F., P. Alström, and D. Engelbrecht. 2017. Possible mechanisms of substrate colour-matching in larks (Alaudidae) and their taxonomic implications. Ibis 159:699–702.

Doucet, S. M., and G. E. Hill. 2009. Do museum specimens accurately represent wild birds? A case study of carotenoid, melanin, and structural colours in long-tailed manakins *Chiroxiphia linearis* . Journal of Avian Biology 40:146–156.

Endler, J. A. 1978. A Predator's View of Animal Color Patterns. Evolutionary Biology 319–364.

Farkas, T. E., T. Mononen, A. A. Comeault, I. Hanski, and P. Nosil. 2013. Evolution of camouflage drives rapid ecological change in an insect community. Current Biology 23:1835–1843.

Fick, S. E., and R. J. Hijmans. 2017. WorldClim 2: new 1-km spatial resolution climate surfaces for global land areas. International Journal of Climatology 37:4302–4315.

Gaston, K. J., S. L. Chown, and K. L. Evans. 2008. Ecogeographical rules: elements of a synthesis. Journal of Biogeography 35:483–500.

Gates, D. 1980. Solar Radiation. Biophysical Ecology, Springer Advanced Texts in Life Sciences. Springer, New York, NY.

Gloger, C. W. L. 1833. Das Abändern der Vögel durch Einfluss des Klimas. August Schulz, Breslau, Germany.

Godfrey, D., J. N. Lythgoe, and D. A. Rumball. 1987. Zebra stripes and tiger stripes: the spatial frequency distribution of the pattern compared to that of the background is significant in display and crypsis. Biological Journal of the Linnean Society 32:427–433.

Gueymard, C. A. 2001. Parameterized transmittance model for direct beam and circumsolar spectral irradiance. Solar Energy 71:325–346.

Gunderson, A. R., E. A. Riddell, M. W. Sears, and E. B. Rosenblum. 2022. Thermal Costs and Benefits of Replicated Color Evolution in the White Sands Desert Lizard Community. The American Naturalist 199:666–678.

Hartman, C. A., and L. W. Oring. 2003. Orientation and microclimate of horned lark nests: the importance of shade. The Condor 105:158–163.

Hijmans, R. J., S. E. Cameron, J. L. Parra, P. G. Jones, and A. Jarvis. 2005. Very high resolution interpolated climate surfaces for global land areas. International Journal of Climatology 25:1965–1978.

Isaac, L. A., and P. T. Gregory. 2013. Can snakes hide in plain view? Chromatic and achromatic crypsis of two colour forms of the Western Terrestrial Garter Snake (Thamnophis elegans). Biological Journal of the Linnean Society 108:756–772.

Kearney, M. R., and W. P. Porter. 2020. NicheMapR – an R package for biophysical modelling: the ectotherm and Dynamic Energy Budget models. Ecography 43:85–96.

Kearney, M. R., W. P. Porter, and S. A. Murphy. 2016. An estimate of the water budget for the endangered night parrot of Australia under recent and future climates. Climate Change Responses 3:14.

Kettlewell, H. B. D. 1955. Selection experiments on industrial melanism in the Lepidoptera. Heredity 9:323–342.

Koskenpato, K., A. Lehikoinen, C. Lindstedt, and P. Karell. 2020. Gray plumage color is more cryptic than brown in snowy landscapes in a resident color polymorphic bird. Ecology and Evolution 10:1751–1761.

Krah, F.-S., U. Büntgen, H. Schaefer, J. Müller, C. Andrew, L. Boddy, J. Diez, et al. 2019. European mushroom assemblages are darker in cold climates. Nature Communications 10:2890.

Laurent, S., S. P. Pfeifer, M. L. Settles, S. S. Hunter, K. M. Hardwick, L. Ormond, V. C. Sousa, et al. 2016. The population genomics of rapid adaptation: disentangling

signatures of selection and demography in white sands lizards. Molecular Ecology 25:306–323.

Lind, O., M. Mitkus, P. Olsson, and A. Kelber. 2013. Ultraviolet sensitivity and colour vision in raptor foraging. Journal of Experimental Biology 216:3764–3764.

Linnen, C. R., E. P. Kingsley, J. D. Jensen, and H. E. Hoekstra. 2009. On the origin and spread of an adaptive allele in deer mice. Science 325:1095–1098.

Maia, R., C. M. Eliason, P.-P. Bitton, S. M. Doucet, and M. D. Shawkey. 2013. pavo : an R package for the analysis, visualization and organization of spectral data. (A. Tatem, ed.)Methods in Ecology and Evolution n/a-n/a.

Maia, R., H. Gruson, J. A. Endler, and T. E. White. 2019. PAVO 2: New tools for the spectral and spatial analysis of colour in R. (R. B. O'Hara, ed.)Methods in Ecology and Evolution 10:1097–1107.

Marcondes, R. S., and R. T. Brumfield. 2020. A simple index to quantify and compare the magnitude of intraspecific geographic plumage colour variation in typical antbirds (Aves: Passeriformes: Thamnophilidae). Biological Journal of the Linnean Society 8.

Marcondes, R. S., J. A. Nations, G. F. Seeholzer, and R. T. Brumfield. 2021. Rethinking Gloger's Rule: Climate, Light Environments, and Color in a Large Family of Tropical Birds (Furnariidae). The American Naturalist 197:592–606.

Marcondes, R. S., K. F. Stryjewski, and R. T. Brumfield. 2020. Testing the simple and complex versions of Gloger's rule in the Variable Antshrike (Thamnophilus caerulescens, Thamnophilidae). The Auk 137:ukaa026.

Marti, C. D., and C. E. Braun. 1975. Use of Tundra Habitats by Prairie Falcons in Colorado. The Condor 77:213–214.

Martin, G., and D. Osorio. 2008. Vision in birds. Pages 22–52 *in* D. Masland and R. Albright, eds. The Sense: A Comprehensive Reference (Vol. 1). Academic Press, San Diego, CA.

Mason, N. A., and R. C. K. Bowie. 2020. Plumage patterns: Ecological functions, evolutionary origins, and advances in quantification. The Auk ukaa060.

Mason, N. A., P. Pulgarin, C. D. Cadena, and I. J. Lovette. 2020. *De novo* assembly of a high-quality reference genome for the Horned Lark (*Eremophila alpestris*). G3:Genes|Genomes|Genetics 10:475–478.

Mason, N. A., P. O. Title, C. Cicero, K. J. Burns, and R. C. K. Bowie. 2014. Genetic variation among western populations of the Horned Lark (*Eremophila alpestris*) indicates recent colonization of the Channel Islands off southern California, mainland-bound dispersal, and postglacial range shifts. The Auk 131:162–174.

Mason, N. A., and P. Unitt. 2018. Rapid phenotypic change in a native bird population following conversion of the Colorado Desert to agriculture. Journal of Avian Biology 49:jav-01507.

Mason, N. A., P. Unitt, and J. P. Sparks. 2021. Agriculture induces isotopic shifts and niche contraction in Horned Larks (Eremophila alpestris) of the Colorado Desert. Journal of Ornithology 162:381–393.

Mason, N., E. Riddell, F. Romero, C. Cicero, and Bowie, RCK. 2022. Data and code for the manuscript “Plumage balances camouflage and thermoregulation in Horned

Larks (Eremophila alpestris).” American Naturalist, Dryad Data Repository https://doi.org/10.6078/D1ZX4S.

Medina, I., E. Newton, M. R. Kearney, R. A. Mulder, W. P. Porter, and D. Stuart-Fox. 2018. Reflection of near-infrared light confers thermal protection in birds. Nature Communications 9:3610.

Merilaita, S., and J. Lind. 2005. Background-matching and disruptive coloration, and the evolution of cryptic coloration. Proceedings of the Royal Society B 272:665–670.

Merilaita, S., J. Tuomi, and V. Jormalainen. 1999. Optimization of cryptic coloration in heterogeneous habitats. Biological Journal of the Linnean Society 67:151–161.

Michalis, C., N. E. Scott-Samuel, D. P. Gibson, and I. C. Cuthill. 2017. Optimal background matching camouflage. Proceedings of the Royal Society B 284.

Nachman, M. W., H. E. Hoekstra, and S. D’Agostino. 2003. The genetic basis of adaptive melanism in pocket mice. Proceedings of the National Academy of Sciences of the USA 100:5268–5273.

Negro, J. J., I. Galván, and J. Potti. 2019. Adaptive plumage wear for increased crypsis in the plumage of Palearctic larks (Alaudidae). Ecology 100:e02771.

Newell, C., H. Walker, and T. Caro. 2021. Pig pigmentation: testing Gloger’s rule. (D. Ge, ed.)Journal of Mammalogy 102:1525–1535.

Owens, P., and E. Rutledge. 2005. Morphology. *in* D. Hillel, ed. Encyclopedia of Soils in the Environment (Vol. 1). Elsevier, Oxford, England.

Porter, W. P., and D. M. Gates. 1969. Thermodynamic Equilibria of Animals with Environment. Ecological Monographs 39:227–244.

Pyle, P. 1997. Identification Guide to North American Birds. Part I: Columbidae to Ploceidae. Braun-Brumfield, Ann Arbor, Michigan.

R Core Team. 2021. R: A language and environment for statistical computing. R Foundation for Statistical Computing, Vienna, Austria.

Riddell, E. A., K. J. Iknayan, B. O. Wolf, B. Sinervo, and S. R. Beissinger. 2019. Cooling requirements fueled the collapse of a desert bird community from climate change. Proceedings of the National Academy of Sciences of the USA 201908791.

Rogalla, S., M. D. Shawkey, and L. D'Alba. 2022. Thermal effects of plumage coloration. Ibis ibi.13100.

Rosenblum, E. B., H. Rompler, T. Schoneberg, and H. E. Hoekstra. 2010. Molecular and functional basis of phenotypic convergence in white lizards at White Sands. Proceedings of the National Academy of Sciences 107:2113–2117.

Sanderman, J., T. Hengl, and G. J. Fiske. 2017. Soil carbon debt of 12,000 years of human land use. Proceedings of the National Academy of Sciences of the USA 114:9575–9580.

Schneider, C. A., W. S. Rasband, and K. W. Eliceiri. 2012. NIH Image to ImageJ: 25 years of image analysis. Nature Methods 9:671–675.

Shakya, S. B., C. Y. Wang-Claypool, C. Cicero, R. C. K. Bowie, and N. A. Mason. 2022. Neo-sex chromosome evolution and phenotypic differentiation across an elevational gradient in horned larks (*Eremophila alpestris*). Molecular Ecology mec.16357.

Shawkey, M. D., B. Igic, S. Rogalla, J. Goldenberg, S. Clusella-Trullas, and L. D'Alba. 2017. Beyond colour: consistent variation in near infrared and solar reflectivity in sunbirds (Nectariniidae). The Science of Nature 104:78.

Shultz, A. J., and K. J. Burns. 2017. The role of sexual and natural selection in shaping patterns of sexual dichromatism in the largest family of songbirds (Aves: Thraupidae). Evolution 71:1061–1074.

Smith, D. G., and J. R. Murphy. 1973. Late summer food habits of adult Burrowing Owls in central Utah. Raptor Research 7:112–115.

Smith, K. R., V. Cadena, J. A. Endler, M. R. Kearney, W. P. Porter, and D. Stuart-Fox. 2016. Color Change for Thermoregulation versus Camouflage in Free-Ranging Lizards. The American Naturalist 188:668–678.

Steel, R., J. Torrie, and D. Dickey. 1997. Principles and Procedures of Statistics: A Biometrical Approach. McGraw-Hill.

Stevens, M., A. E. Lown, and L. E. Wood. 2014. Color change and camouflage in juvenile shore crabs Carcinus maenas. Frontiers in Ecology and Evolution 2:1–14.

Stevens, M., and S. Merilaita. 2009. Animal camouflage: current issues and new perspectives. Philosophical Transactions of the Royal Society B 364:423–427.

Stevens, M., J. Troscianko, J. K. Wilson-Aggarwal, and C. N. Spottiswoode. 2017. Improvement of individual camouflage through background choice in ground-nesting birds. Nature Ecology & Evolution 1:1325–1333.

Stoddard, M. C., and D. Osorio. 2019. Animal coloration patterns: linking spatial vision to quantitative analysis. The American Naturalist 193:164–186.

Stoddard, M. C., and R. O. Prum. 2008. Evolution of avian plumage color in a tetrahedral color space: a phylogenetic analysis of New World buntings. The American Naturalist 171:755–776.

Stoddard, M. C., and M. Stevens. 2010. Pattern mimicry of host eggs by the Common Cuckoo, as seen through a bird's eye. Proceedings of the Royal Society B 277:1387–1393.

Stuart-Fox, D., and A. Moussalli. 2009. Camouflage, communication and thermoregulation: lessons from colour changing organisms. Philosophical Transactions of the Royal Society B: Biological Sciences 364:463–470.

Stuart-Fox, D., E. Newton, and S. Clusella-Trullas. 2017. Thermal consequences of colour and near-infrared reflectance. Philosophical Transactions of the Royal Society B 372:20160345.

Stuart-Fox, D., E. Newton, R. A. Mulder, L. D'Alba, M. D. Shawkey, and B. Igic. 2018. The microstructure of white feathers predicts their visible and near-infrared reflectance properties. (D. Osorio, ed.) PLOS ONE 13:e0199129.

Tieleman, B. I., J. B. Williams, and P. Bloomer. 2003*a*. Adaptation of metabolism and evaporative water loss along an aridity gradient. Proceedings of the Royal Society B 270:207–214.

Tieleman, B. I., J. B. Williams, and M. E. Buschur. 2002. Physiological Adjustments to Arid and Mesic Environments in Larks (*Alaudidae*). Physiological and Biochemical Zoology 75:305–313.

Tieleman, B. I., J. B. Williams, M. E. Buschur, and C. R. Brown. 2003*b*. Phenotypic variation of larks along an aridity gradient: are desert birds more flexible? Ecology 84:1800–1815.

Troscianko, J., and M. Stevens. 2015. Image calibration and analysis toolbox - a free software suite for objectively measuring reflectance, colour and pattern. (S. Rands, ed.)Methods in Ecology and Evolution 6:1320–1331.

Troscianko, J., J. Wilson-Aggarwal, M. Stevens, and C. N. Spottiswoode. 2016. Camouflage predicts survival in ground-nesting birds. Scientific Reports 6:19966.

Trost, C. H. 1972. Adaptations of Horned Larks (Eremophila alpestris) to Hot Environments. The Auk 89:506–527.

Van't Hof, A. E., N. Edmonds, M. Dalíková, F. Marec, and I. J. Saccheri. 2011. Industrial melanism in british peppered moths has a singular and recent mutational origin. Science 332:958–960.

Verbeek, N. A. M. 1967. Breeding Biology and Ecology of the Horned Lark in Alpine Tundra. The Wilson Bulletin 79:208–218.

Vignieri, S. N., J. G. Larson, and H. E. Hoekstra. 2010. The selective advantage of crypsis in mice. Evolution 64:2153–2158.

Vo, A.-T. E., M. S. Bank, J. P. Shine, and S. V. Edwards. 2011. Temporal increase in organic mercury in an endangered pelagic seabird assessed by century-old museum specimens. Proceedings of the National Academy of Sciences of the USA 108:7466–7471.

Vorobyev, M., D. Osorio, A. T. D. Bennett, N. J. Marshall, and I. C. Cuthill. 1998. Tetrachromacy, oil droplets and bird plumage colours. Journal of Comparative Physiology A: Sensory, Neural, and Behavioral Physiology 183:621–633.

Wacker, C. B., B. M. McAllan, G. Körtner, and F. Geiser. 2016. The functional requirements of mammalian hair: a compromise between crypsis and thermoregulation? The Science of Nature 103:53.

Walde, A. D., A. M. Walde, D. K. Delaney, and L. L. Pater. 2009. Burrows of Desert Tortoises (Gopherus agassizii) as Thermal Refugia for Horned Larks (Eremophila alpestris) in the Mojave Desert. The Southwestern Naturalist 54:375–381.

Walsberg, G. E. 1983. Coat Color and Solar Heat Gain in Animals. BioScience 33:88–91.

———. 1988. Heat flow through avian plumages: The relative importance of conduction, convection, and radiation. Journal of Thermal Biology 13:89–92.

Wiens, J. A., J. T. Rotenberry, and B. V. Horne. 1987. Habitat Occupancy Patterns of North American Shrubsteppe Birds: The Effects of Spatial Scale. Oikos 48:132.

Williams, J. B., B. I. Tieleman, and M. Shobrak. 1999. Lizard Burrows Provide Thermal Refugia for Larks in the Arabian Desert. The Condor 101:714–717.

Wolf, B. O., and G. E. Walsberg. 2000. The Role of the Plumage in Heat Transfer Processes of Birds. American Zoologist 40:575–584.

Zink, R. M., and J. V. Remsen. 1986. Evolutionary Processes and Patterns of Geographic Variation in Birds. Current Ornithology 4:1–69.

Tables

Table 1: Linear model output for plumage-soil associations. *P*-values with asterisks indicate statistically significant terms (*$P < 0.05$; **$P < 0.01$; ***$P < 0.001$), but significance is not shown for intercept terms. Plots of these data are shown in Figure 2.

Response Variable	Predictor Variable	Beta + SE	t-value	*P*-value
Dorsal Brightness	(Intercept)	4.95e-03 ± 2.67e+01	26.68	1.90e-70
	Soil PC1 (Brightness)	6.51e-05 ± 1.77e+00	1.77	7.87e-02
	Soil PC2 (Redness)	2.18e-04 ± -9.38e-02	-0.09	9.25e-01
	Soil Granularity	2.33e-04 ± 7.49e+00	7.49	1.74e-12***
	Bioclim PC2 (Aridity)	6.76e-06 ± 9.00e+00	9	1.17e-16***
	Bioclim PC3 (Temperature)	1.66e-05 ± 5.41e+00	5.41	1.69e-07***
	Sex_{male}	3.24e-03 ± 1.44e+00	1.44	1.53e-01
	Years Since Collection	6.23e-05 ± 1.76e+00	1.76	7.98e-02
Achieved Chroma	(Intercept)	6.03e-03 ± 4.94e+01	49.39	5.30e-120
	Soil PC1 (Brightness)	7.92e-05 ± -2.23e-02	-0.02	9.82e-01
	Soil PC2 (Redness)	2.66e-04 ± 5.56e+00	5.56	8.01e-08***
	Soil Granularity	2.83e-04 ± 1.38e+00	1.38	1.68e-01
	Bioclim PC2 (Aridity)	8.23e-06 ± -7.37e-01	-0.74	4.62e-01
	Bioclim PC3 (Temperature)	2.02e-05 ± 3.18e+00	3.18	1.71e-03**
	Sex_{male}	3.94e-03 ± 3.39e-01	0.34	7.35e-01
	Years Since Collection	7.58e-05 ± 1.94e+00	1.94	5.36e-02
Hue (theta)	(Intercept)	1.02e-02 ± 2.29e+01	22.92	7.08e-60
	Soil PC1 (Brightness)	1.34e-04 ± 1.62e-01	0.16	8.72e-01
	Soil PC2 (Redness)	4.51e-04 ± -4.79e+00	-4.79	3.15e-06***

	Soil Granularity	4.81e-04 ± -6.07e+00	-6.07	5.63e-09***
	Bioclim PC2 (Aridity)	1.40e-05 ± -5.45e+00	-5.45	1.35e-07***
	Bioclim PC3 (Temperature)	3.43e-05 ± -2.47e+00	-2.47	1.42e-02*
	Sex_{male}	6.69e-03 ± -6.84e+00	-6.84	8.11e-11***
	Years Since Collection	1.29e-04 ± -3.70e+00	-3.7	2.76e-04***
Hue (phi)	(Intercept)	7.09e-03 ± -1.18e+02	-117.68	1.47e-198
	Soil PC1 (Brightness)	9.31e-05 ± -1.08e+00	-1.08	2.82e-01
	Soil PC2 (Redness)	3.13e-04 ± 4.26e+00	4.26	3.00e-05***
	Soil Granularity	3.33e-04 ± -2.44e+00	-2.44	1.55e-02*
	Bioclim PC2 (Aridity)	9.67e-06 ± -1.09e+00	-1.09	2.78e-01
	Bioclim PC3 (Temperature)	2.38e-05 ± -1.54e+00	-1.54	1.25e-01
	Sex_{male}	4.63e-03 ± 3.54e+00	3.54	4.89e-04***
	Years Since Collection	8.91e-05 ± 2.46e+00	2.46	1.48e-02*
Dorsal patterning (power)	(Intercept)	4.81e-03 ± 2.39e+01	23.94	8.10e-63
	Soil PC1 (Brightness)	6.31e-05 ± 1.53e+00	1.53	1.28e-01
	Soil PC2 (Redness)	2.12e-04 ± -1.66e+00	-1.66	9.89e-02
	Soil Granularity	2.26e-04 ± 2.39e+00	2.39	1.77e-02*
	Bioclim PC2 (Aridity)	6.56e-06 ± 1.67e+00	1.67	9.67e-02
	Bioclim PC3 (Temperature)	1.61e-05 ± 1.24e+00	1.24	2.17e-01
	Sex_{male}	3.14e-03 ± -4.78e+00	-4.78	3.25e-06***
	Years Since Collection	6.04e-05 ± 8.44e-01	0.84	3.99e-01

Table 2: Non-linear regression analyses for investigating the relationship between the reduction in cooling costs, temperature, and aridity. Slopes and standard errors are presented and correspond to parameters in the exponential function $f(x) = a^{bx}$.

Temperature model	***a***	***b***
Slope ± SE	0.034 ± 0.016	0.006 ± 0.003
t-value	2.12	2.47
p-value	0.04	0.02
Aridity model		
Slope ± SE	0.016 ± 0.008	0.006 ± 0.001
t-value	1.93	4.79
p-value	0.06	< 0.001

Figure Legends

Figure 1: Sampling map showing localities of vouchered Horned Lark (*Eremophila alpestris*) specimens. Soil color is based on USDA soil surveys. The approximate range of each subspecies is shown in a different color based on Behle (1942) and museum records. Some dots may represent more than one individual sampled from the same locality. The number of samples per subspecies is given next to the subspecies in the top-right legend. Distributions and samples of certain subspecies (*alpestris, arcticola, enertera, hoyti, aphrasta*) are not shown because we focused on the geographic area where soil color data are available in the contiguous United States (see Supplementary Figure S1 for complete sampling).

Figure 2: Variation in Horned Lark plumage. A principal component analysis (A) reveals some clustering but substantial overlap among subspecies (colors correspond to labels below the set of boxplots, panels B-K) and between sexes (males shown with squares, females shown with circles). Panels B–K show box plots of brightness, achieved chroma (saturation), hue (theta), hue (phi), and dorsal patterning for males and females. Letters above each boxplot correspond to Tukey's posthoc groupings. Subspecies are ordered to reflect approximate geographic distributions from northwest to southeast. Insets show vouchered specimens, including male and female Horned Larks of various subspecies corresponding to circled points in the scatterplot (A).

Figure 3: Phenotype-environment associations in the dorsal coloration and patterning of Horned Larks in the western United States. The color of each point corresponds to

the subspecies as in Figure 1. Squares correspond to males and circles to females. The P-value for the effect size of each variable from generalized linear models that include soil brightness, soil redness, soil granularity, aridity, temperature, sex, and specimen age as main effects is shown in the upper right hand corner of each plot. A trend line for the relationship between the two variables is drawn when the effect size is significant ($P < 0.05$). Approximate soil color is shown below panels U and V that correspond to soil color PC1 (brightness) and soil color PC2 (redness).

Figure 4: Variation in feather reflectance reduces thermoregulatory costs in hotter locations. Shown are the relationships between climatic principal components and the reduction in water requirements for evaporative cooling (termed cooling costs) due to variation in dorsal feather reflectance. The reduction in cooling costs was not associated with the principal component for (A) seasonality but was associated with (B) aridity and (C) temperature. The analyses suggest that aridity and temperature are major drivers of variation in feather reflectance for thermoregulatory purposes. Exponential models are plotted with 95% confidence intervals in the dotted line.

Figure 5: Scatterplot of residual brightness values from a linear model—which included soil brightness, soil redness, soil granularity, aridity, temperature, sex, and specimen age as main effects—and individual estimates of cooling benefits from our thermoregulatory models based on solar reflectance profiles. Dotted line is a residual value of zero, such that individuals above the dotted line are brighter than expected based on our linear model incorporating environmental conditions. The solid line shows

the estimated trend line between the two plotted variables. Circles correspond to females and squares correspond to males. Colors of each symbol correspond to subspecies as seen in Figure 1.

Figure 1

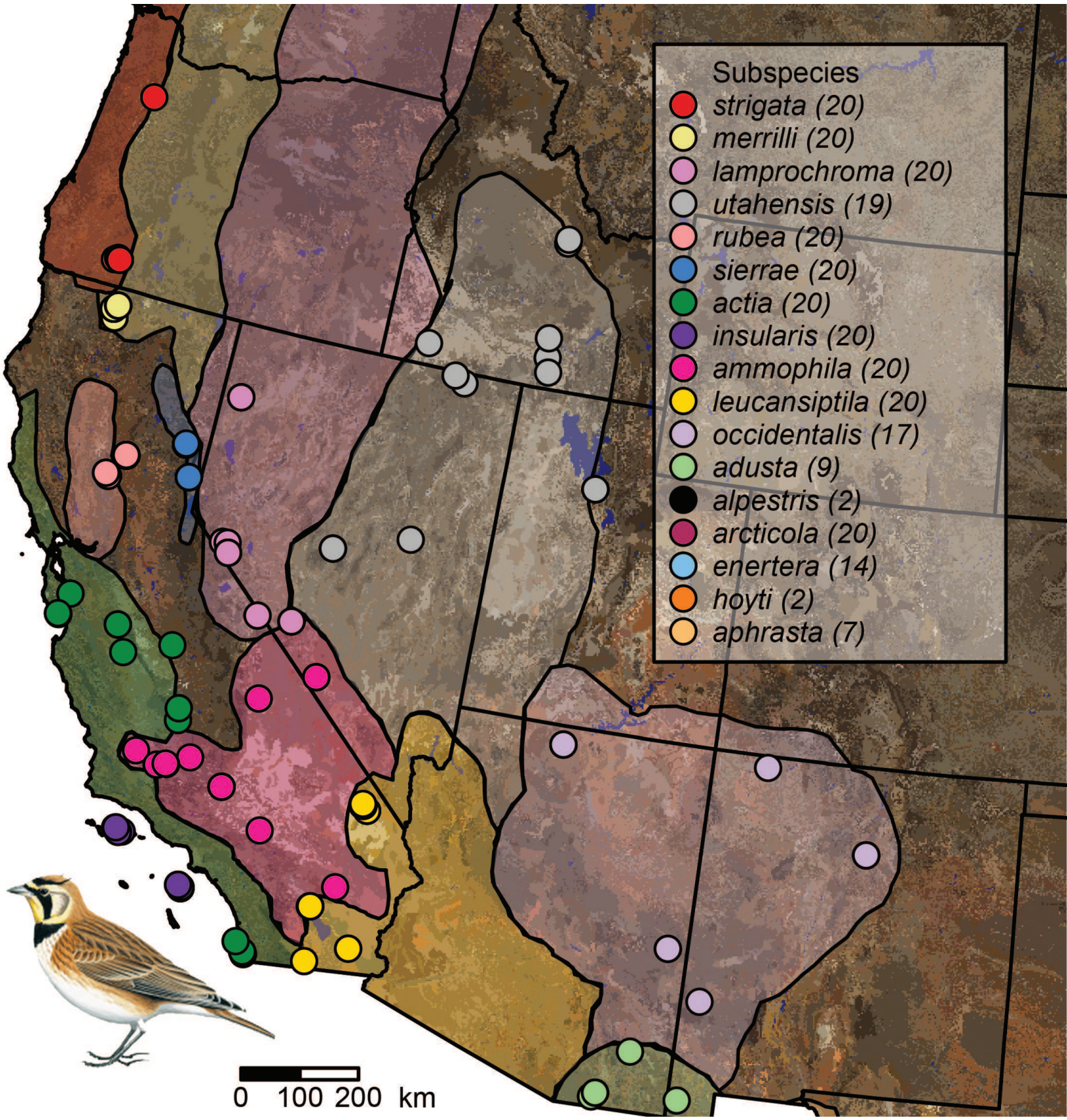

Figure 2

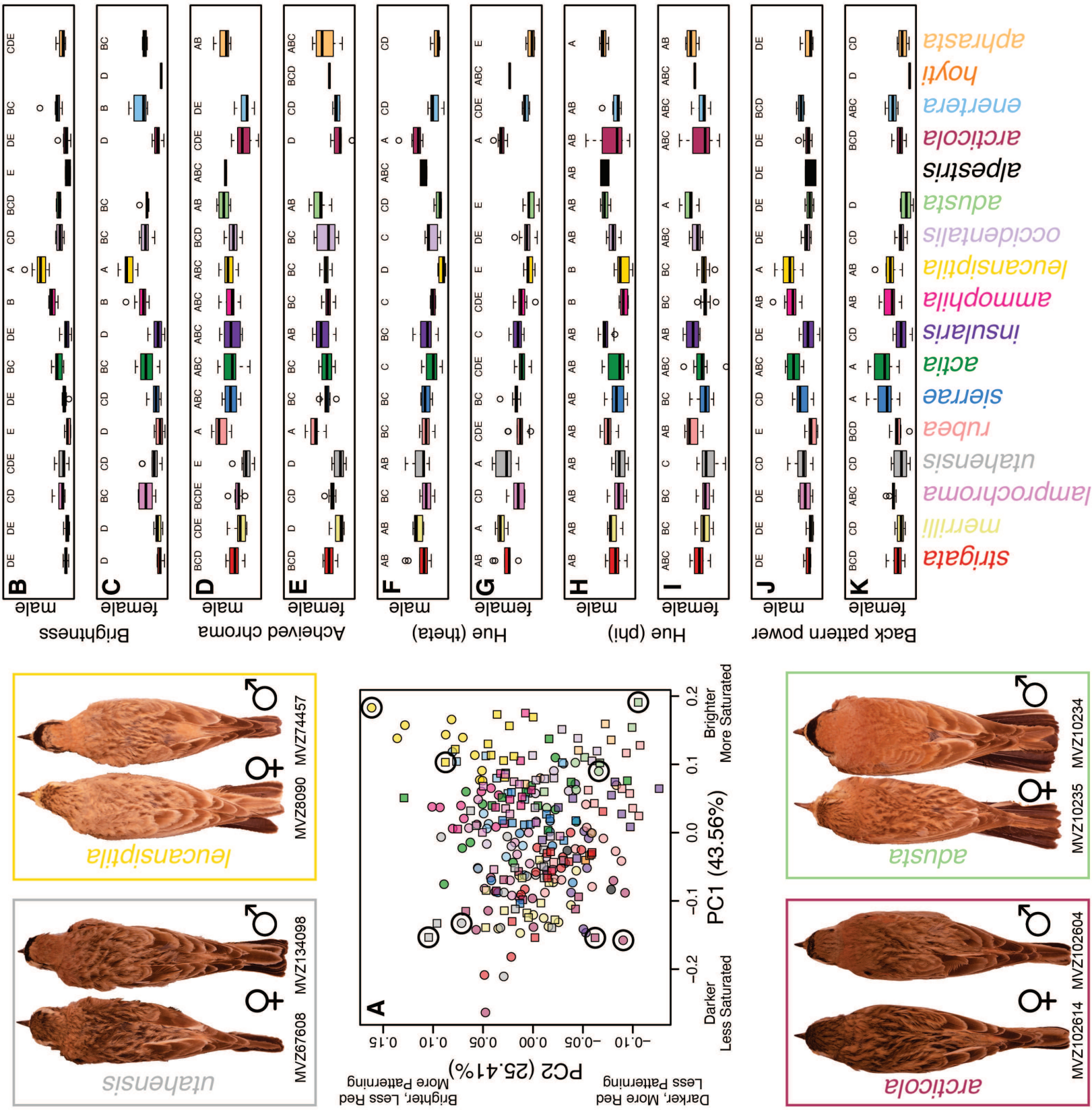

Figure 3

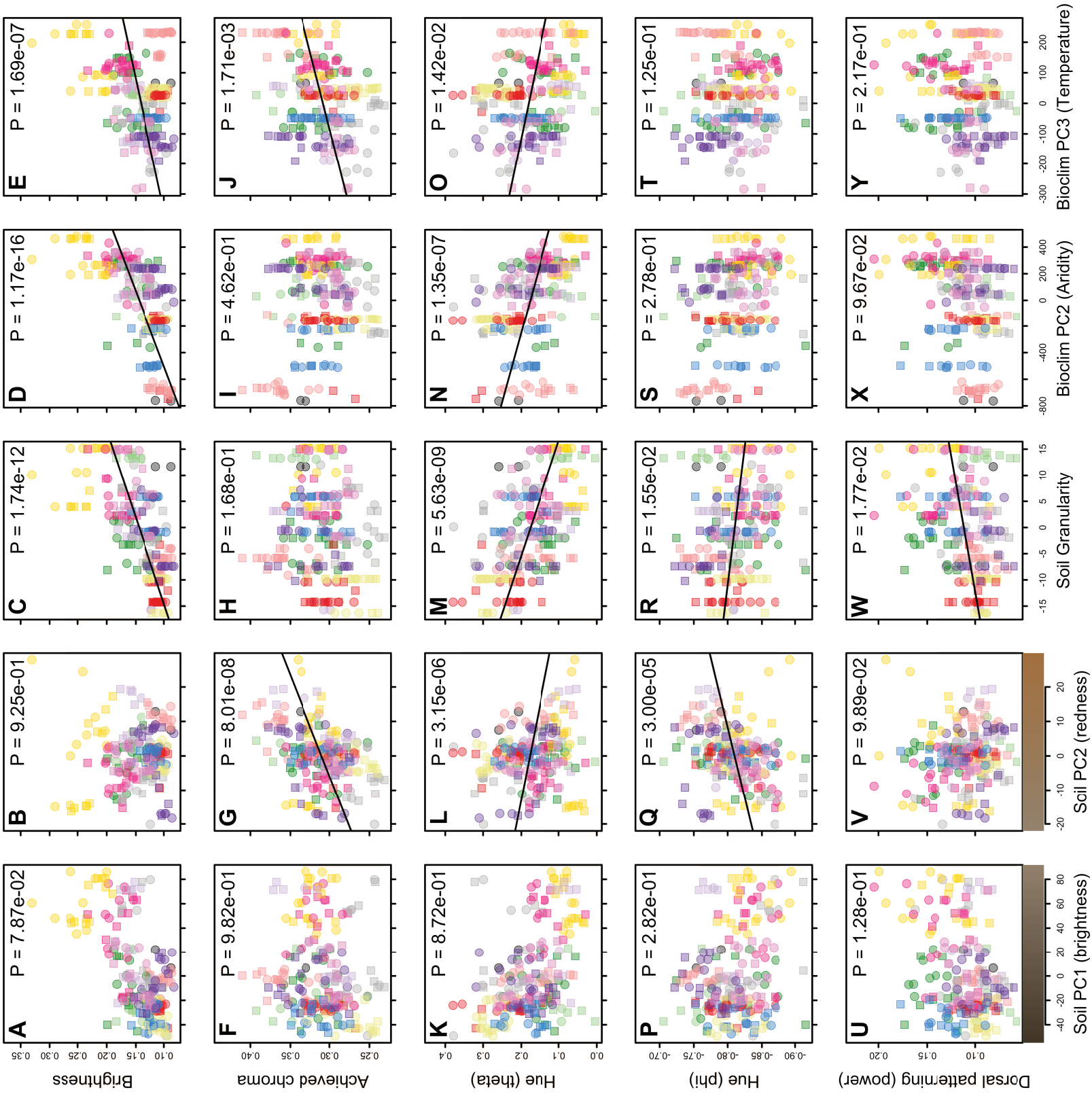

Figure 4

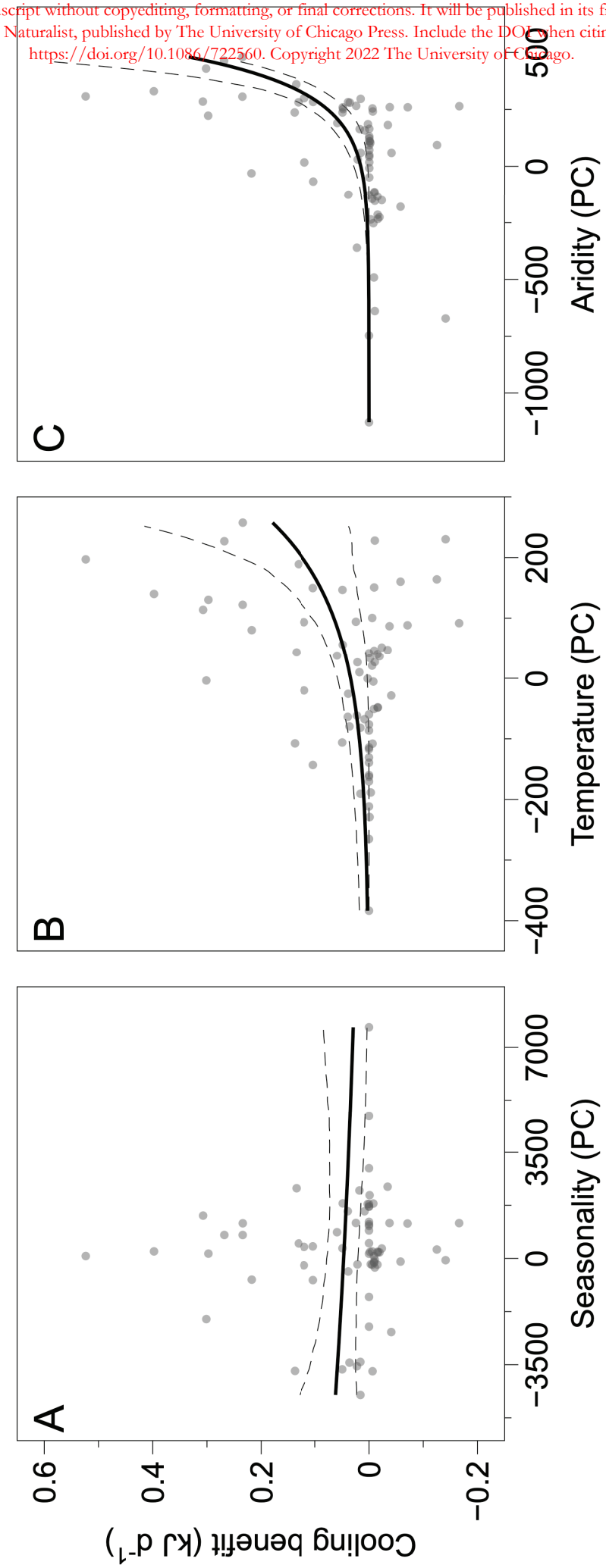

Figure 5

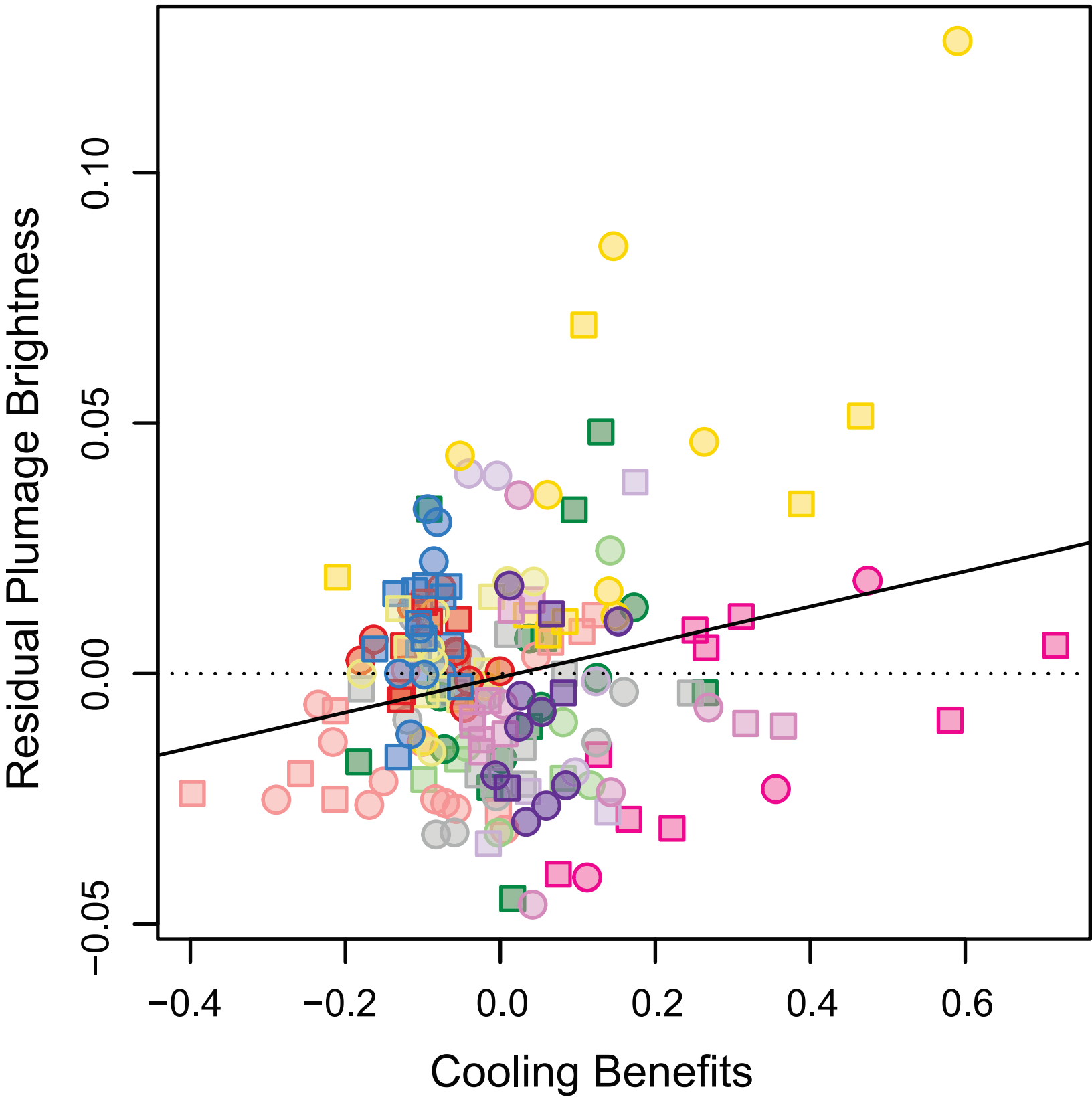

PLUMAGE BALANCES CAMOUFLAGE AND THERMOREGULATION IN HORNED LARKS (*EREMOPHILA ALPESTRIS*)

Nicholas A. Mason[1,2], Eric A. Riddell[1,3], Faye G. Romero[1], Carla Cicero[1], Rauri C.K. Bowie[1,4]

[1]Museum of Vertebrate Zoology, University of California, Berkeley, California, USA
[2]Museum of Natural Science and Department of Biological Sciences, Louisiana State University, Baton Rouge, Louisiana, USA
[3]Iowa State University, Department of Ecology, Evolution, and Organismal Biology, Ames, Iowa, USA
[4]Department of Integrative Biology, University of California, Berkeley, California, USA

*Corresponding author: mason@lsu.edu

Journal Title: The American Naturalist

Supplementary Information

Supplementary Figure S1: Comprehensive sampling map of all vouchered specimens included in this study.
Supplementary Figure S2: Example of photography set up and dorsal region of interest (back).
Supplementary Figure S3: Scatterplot of principal component scores of color metrics, including minimum convex hull polygons for males (dotted lines) and females (solid lines) for each subspecies.
Supplementary Figure S4: Zoomed-in boxplot showing interquartile ranges and variation in mean luminosity among females of Horned Lark from different subspecies.
Supplementary Figure S5: Zoomed-in boxplot showing interquartile ranges and variation in mean luminosity among males of Horned Lark from different subspecies.
Supplementary Figure S6: Zoomed-in boxplot showing interquartile ranges and variation in achieved chroma among females of Horned Lark from different subspecies.
Supplementary Figure S7: Zoomed-in boxplot showing interquartile ranges and variation in achieved chroma among males of Horned Lark from different subspecies.
Supplementary Figure S8: Zoomed-in boxplot showing interquartile ranges and variation in hue (theta) among females of Horned Lark from different subspecies.
Supplementary Figure S9: Zoomed-in boxplot showing interquartile ranges and variation in hue (theta) among males of Horned Lark from different subspecies.
Supplementary Figure S10: Zoomed-in boxplot showing interquartile ranges and variation in hue (phi) among females of Horned Lark from different subspecies.
Supplementary Figure S11: Zoomed-in boxplot showing interquartile ranges and variation in hue (phi) among males of Horned Lark from different subspecies.
Supplementary Figure S12: Zoomed-in boxplot showing interquartile ranges and variation in power (patterning) among females of Horned Lark from different subspecies.
Supplementary Figure S13: Zoomed-in boxplot showing interquartile ranges and variation in power (patterning) among males of Horned Lark from different subspecies.
Supplementary Figure S14: Box plots illustrating differences in plumage characters between female and male Horned Larks.
Supplementary Figure S15: Scatterplots showing each plumage metric considered in this study alongside the years since collection for each specimen.
Supplementary Figure S16: Correlation plot showing pair-wise correlation values between predictor variables included in our linear models of plumage-environment associations.
Supplementary Table S1: Voucher information for 270 individuals of Horned Lark (*Eremophila alpestris*) included in this study.
Supplementary Table S2: Principal component analysis loadings for plumage data set.
Supplementary Table S3: Principal component analysis loadings for soil color data set.
Supplementary Table S4: Principal component analysis loadings for soil granularity data set.
Supplementary Table S5: Principal component analysis loadings for WorldClim bioclimatic data set.
Supplementary Table S6: Model selection for climatic covariates and reduction in cooling costs.

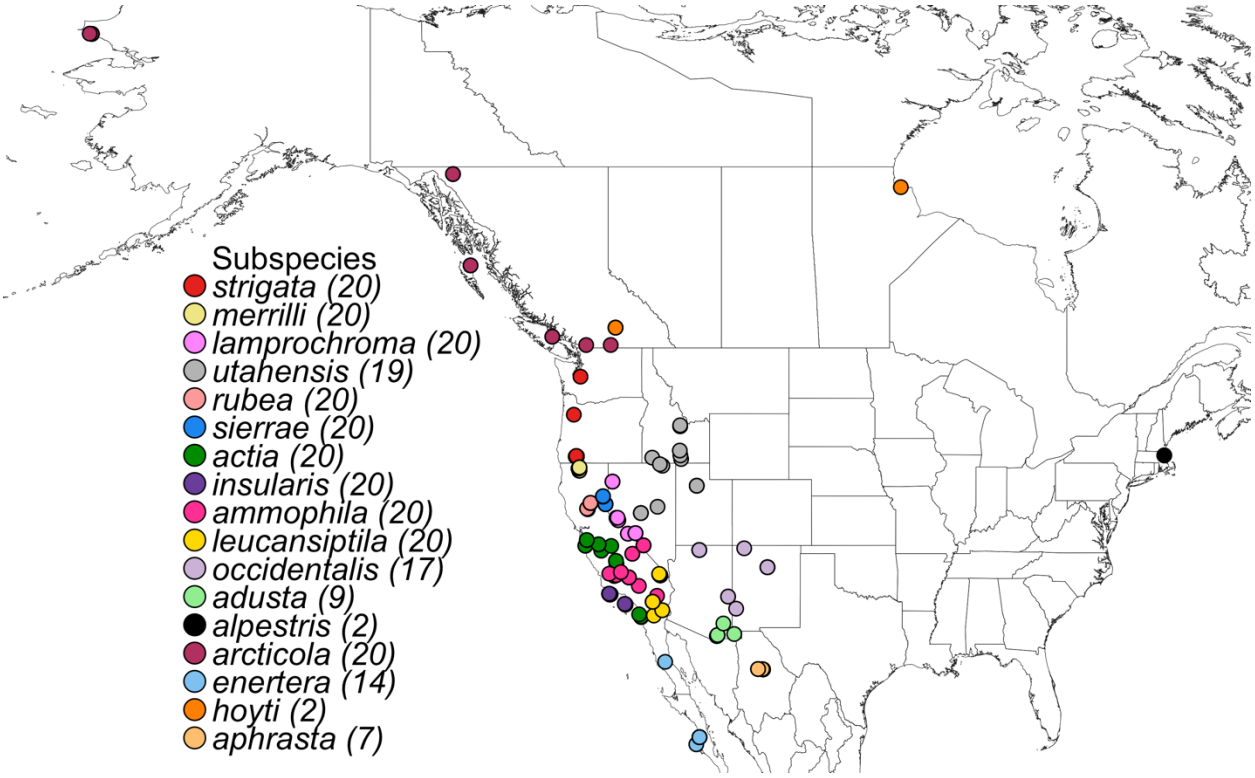

Supplementary Figure S1: Comprehensive sampling map of all vouchered specimens included in this study. Sample sizes are shown in parentheses next to subspecies names on legend on the left side of the figure. Some dots may represent more than one individual taken from the same locality.

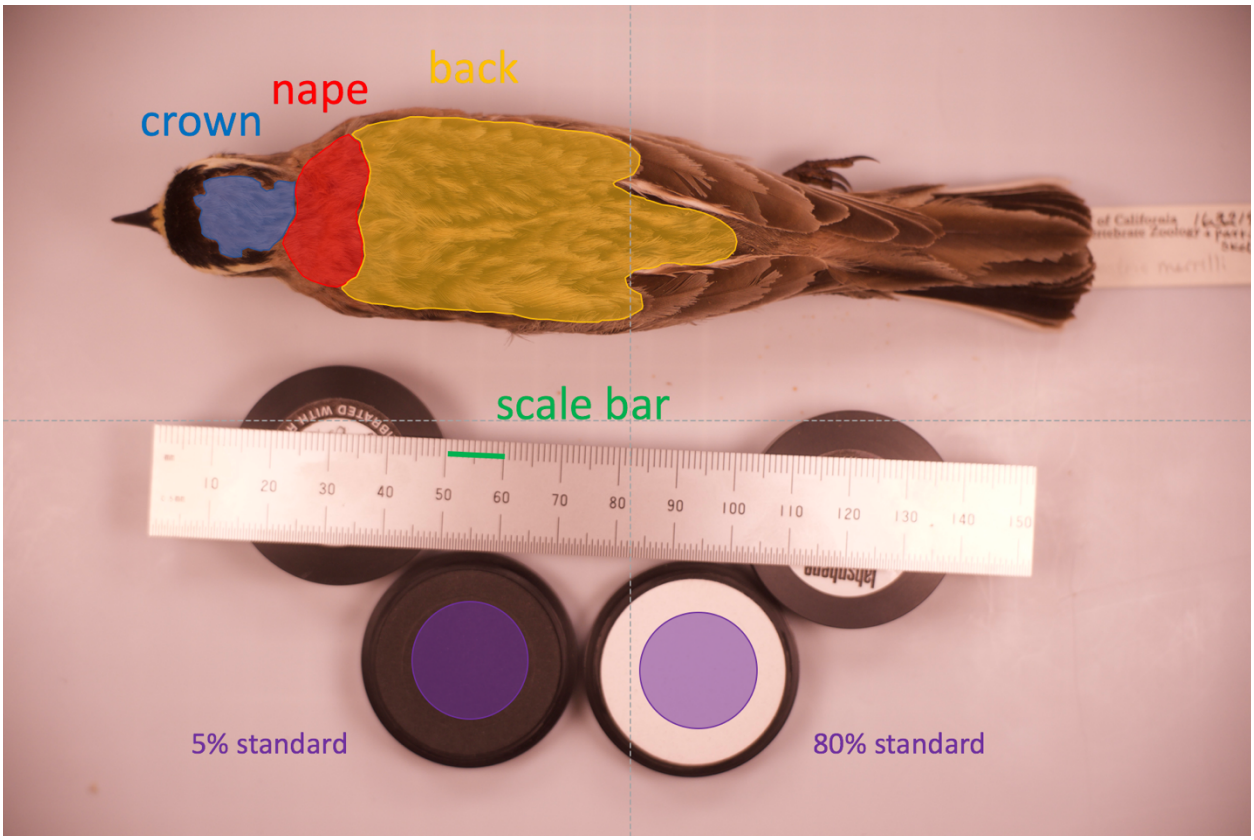

Supplementary Figure S2: Photography setup and example of polygon corresponding to region of interest (back) measured among Horned Larks (*Eremophila alpestris*) in this study.

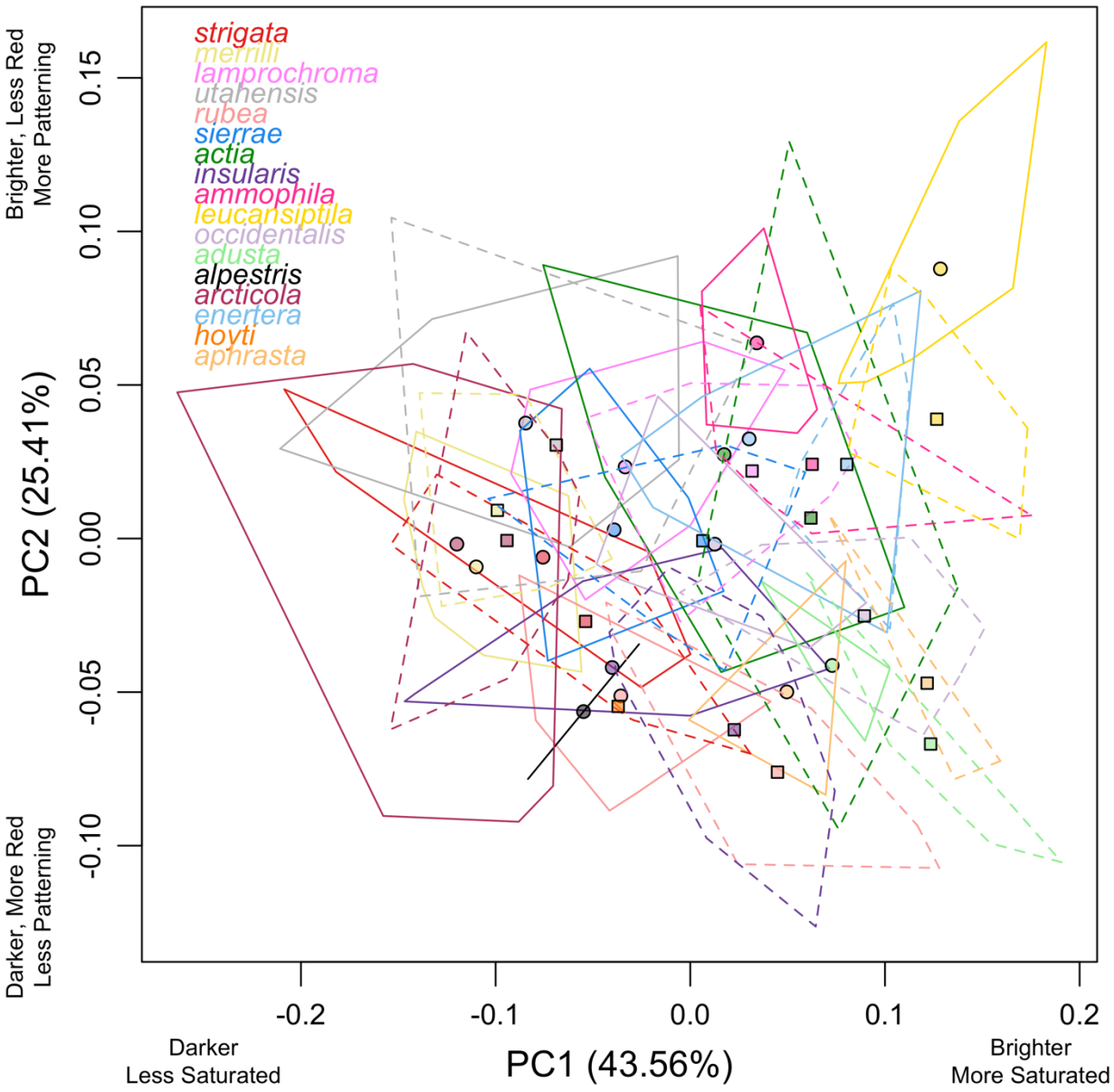

Supplementary Figure S3: Scatterplot of principal component scores of color metrics, including minimum convex hull polygons for males (dotted lines) and females (solid lines) for each subspecies. Average values for each subspecies are shown for males (squares) and females (circles). Colors correspond to each subspecies as shown in the upper left of the plot.

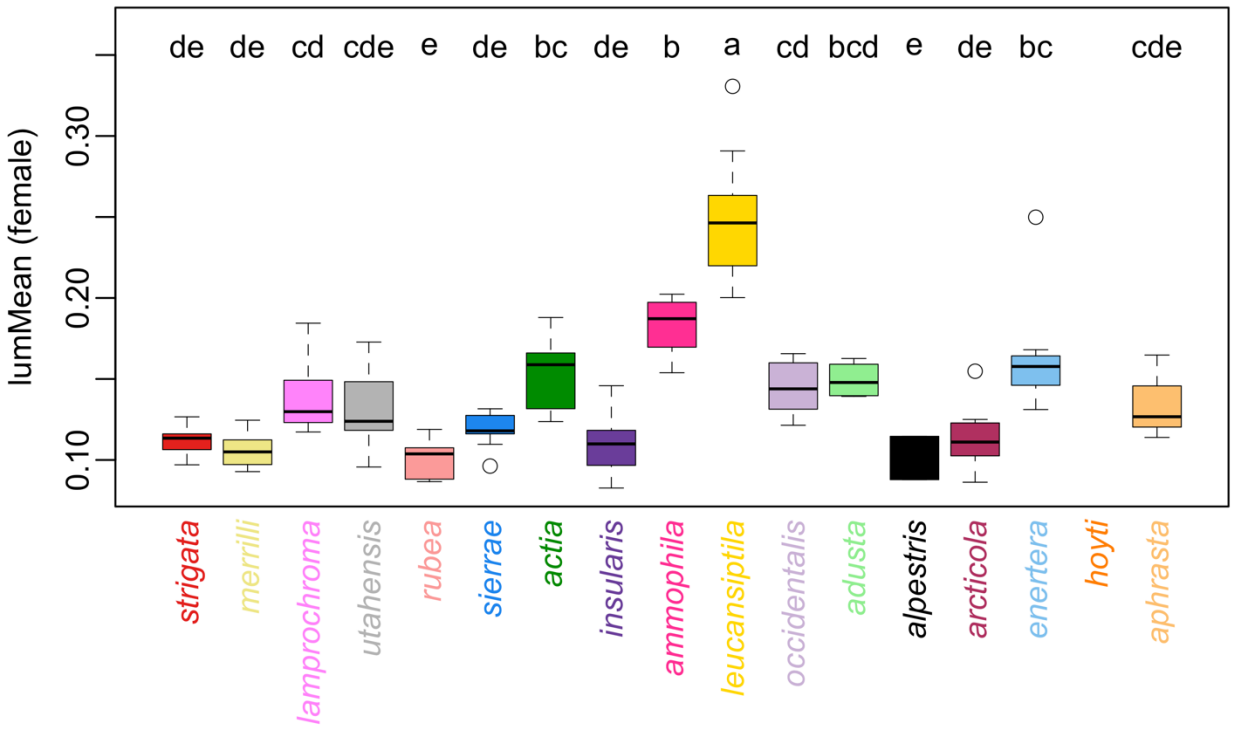

Supplementary Figure S4: Boxplot showing interquartile ranges and variation in mean luminosity among females of different subspecies of Horned Larks. Letters above each plot show the output of a posthoc Tukey's pairwise comparison. Circles represent outliers.

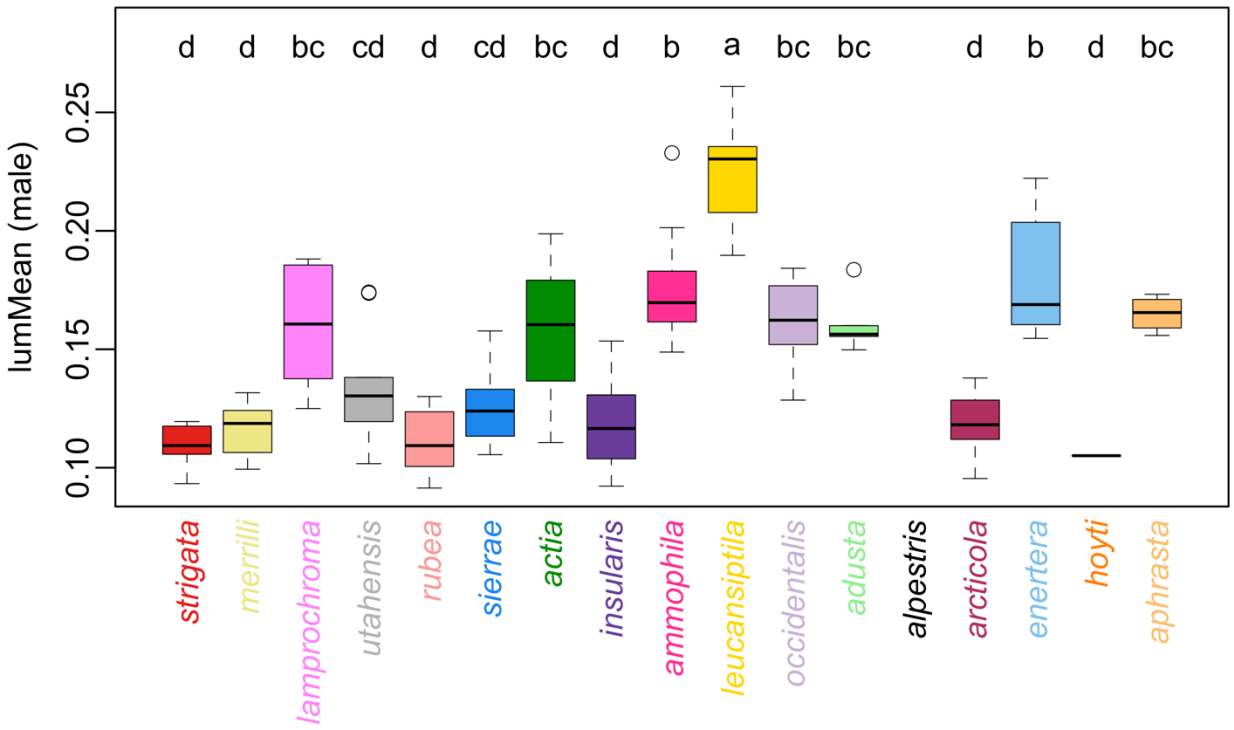

Supplementary Figure S5: Boxplot showing interquartile ranges and variation in mean luminosity among males of different subspecies of Horned Larks. Letters above each plot show the output of a posthoc Tukey's pairwise comparison. Circles represent outliers.

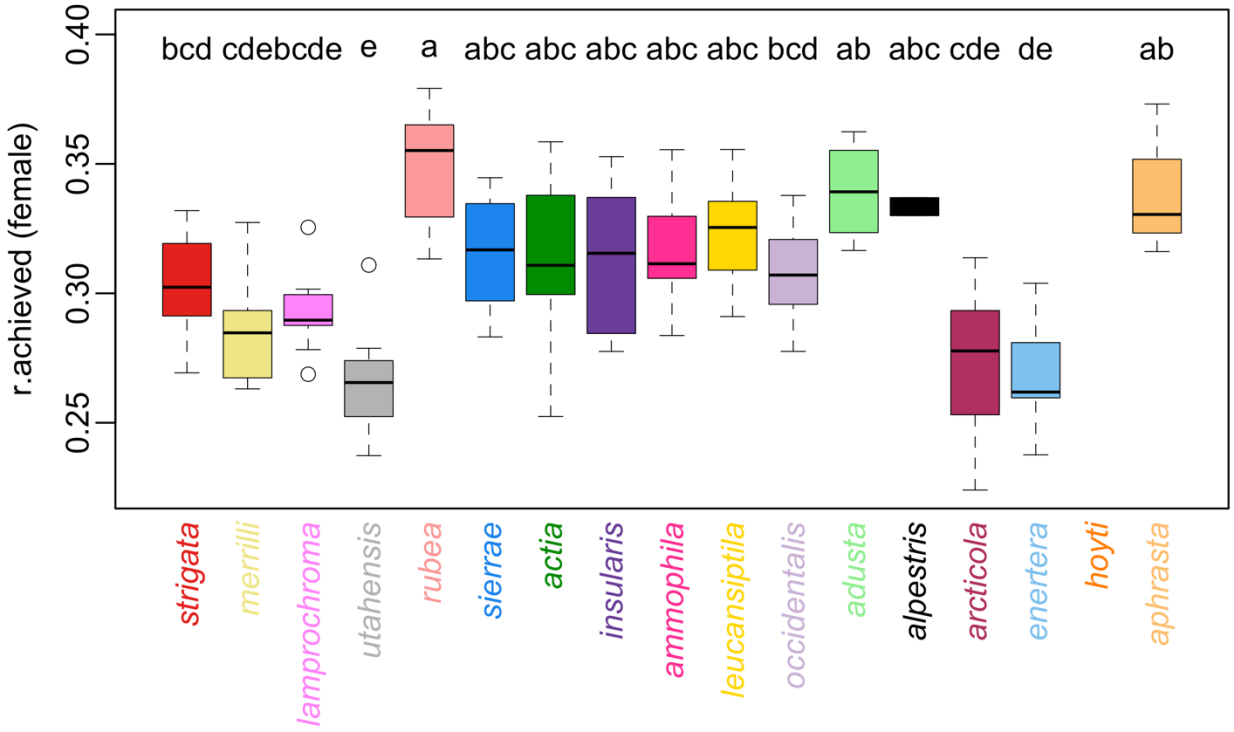

Supplementary Figure S6: Boxplot showing interquartile ranges and variation in achieved chroma among females of different subspecies of Horned Larks. Letters above each plot show the output of a posthoc Tukey's pairwise comparison. Circles represent outliers.

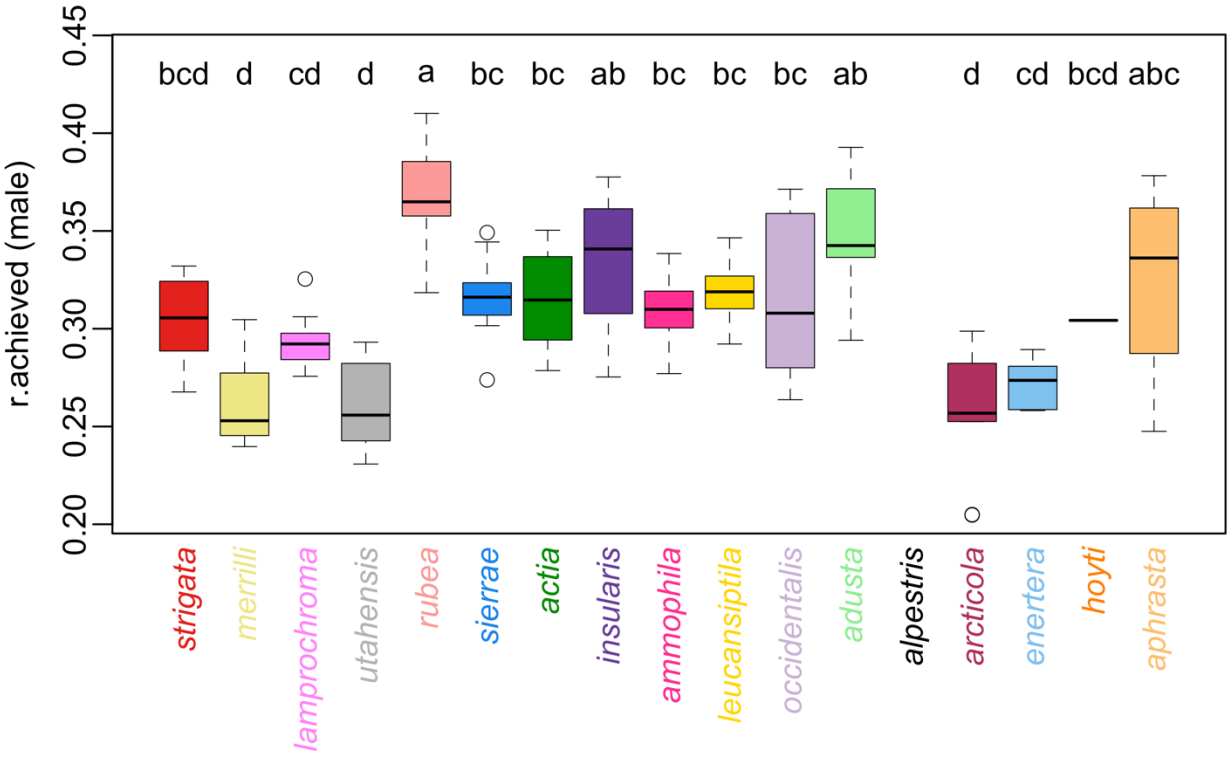

Supplementary Figure S7: Boxplot showing interquartile ranges and variation in achieved chroma among males of different subspecies of Horned Larks. Letters above each plot show the output of a posthoc Tukey's pairwise comparison. Circles represent outliers.

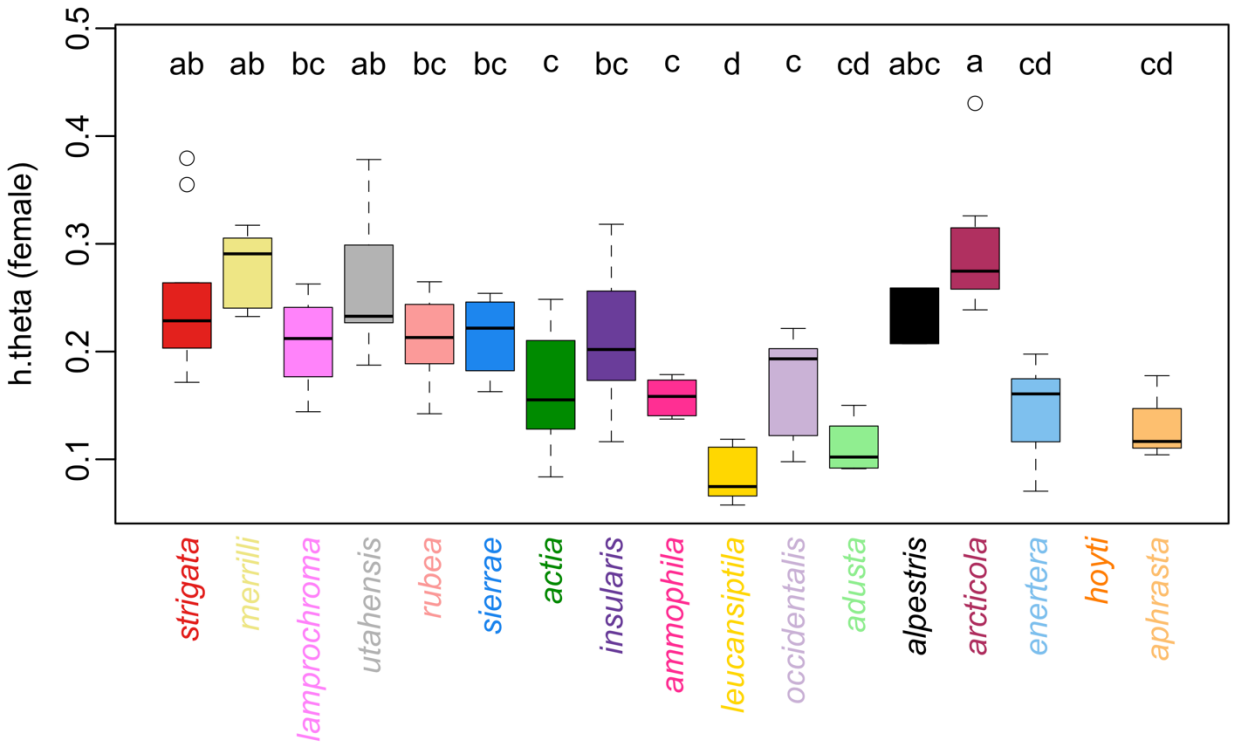

Supplementary Figure S8: Boxplot showing interquartile ranges and variation in hue (theta) among females of different subspecies of Horned Larks. Letters above each plot show the output of a posthoc Tukey's pairwise comparison. Circles represent outliers.

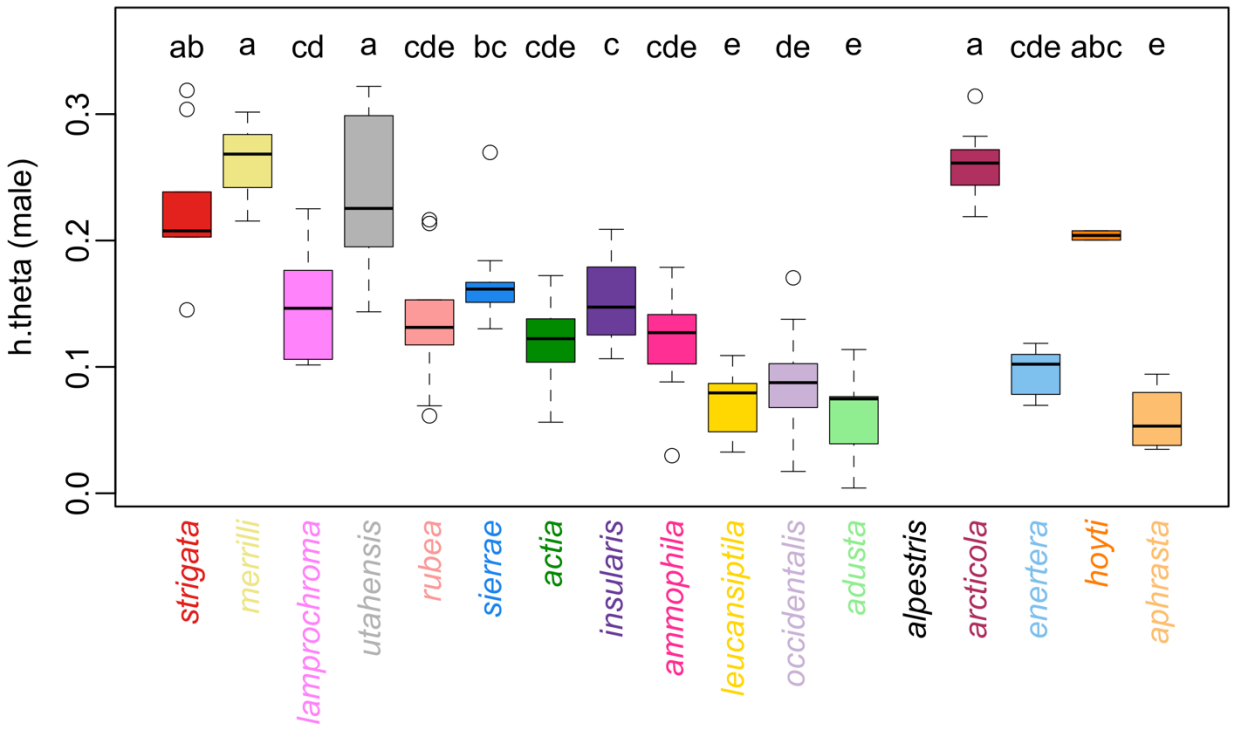

Supplementary Figure S9: Boxplot showing interquartile ranges and variation in hue (theta) among males of different subspecies of Horned Larks. Letters above each plot show the output of a posthoc Tukey's pairwise comparison. Circles represent outliers.

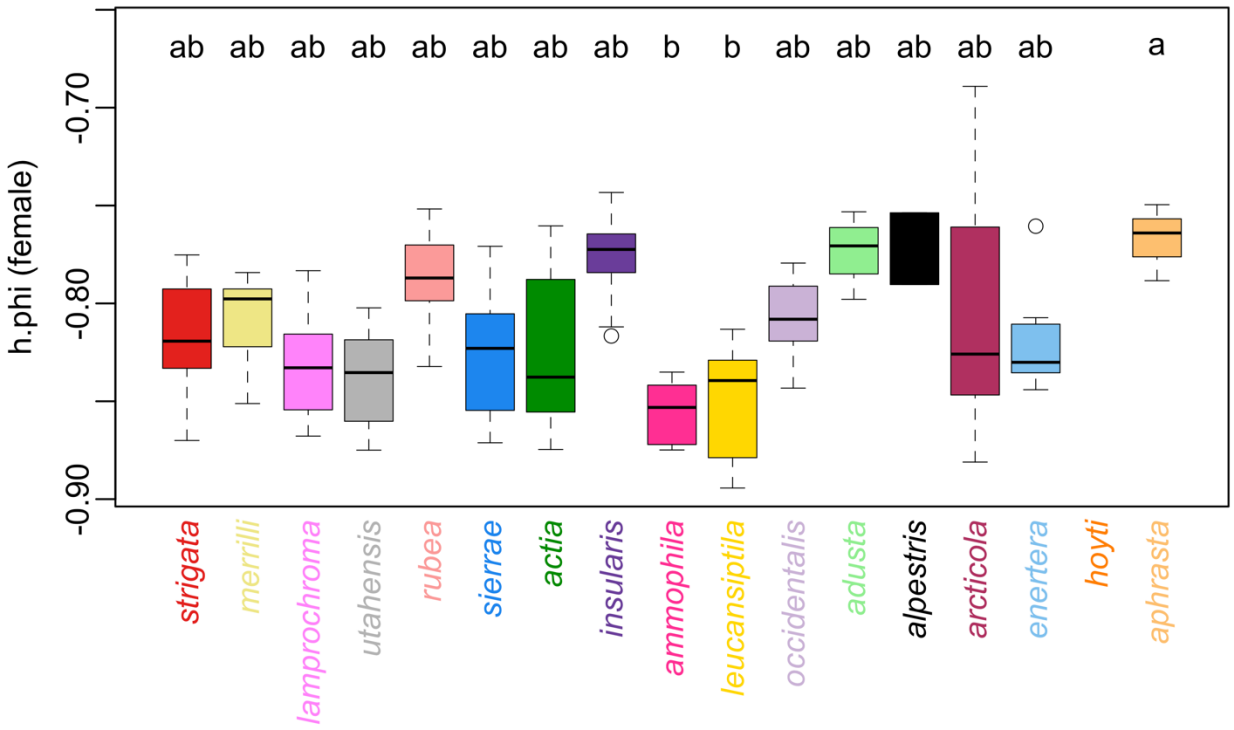

Supplementary Figure S10: Boxplot showing interquartile ranges and variation in hue (phi) among females of different subspecies of Horned Larks. Letters above each plot show the output of a posthoc Tukey's pairwise comparison. Circles represent outliers.

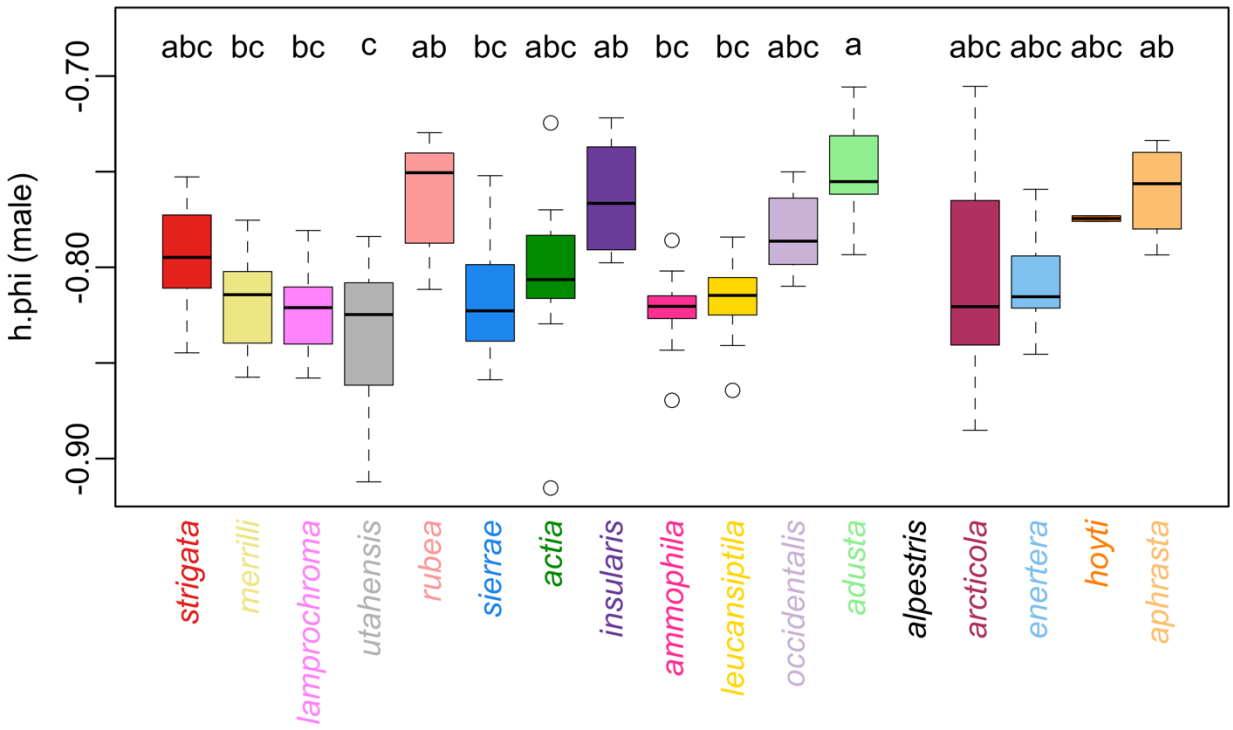

Supplementary Figure S11: Boxplot showing interquartile ranges and variation in hue (phi) among males of different subspecies of Horned Larks. Letters above each plot show the output of a posthoc Tukey's pairwise comparison. Circles represent outliers.

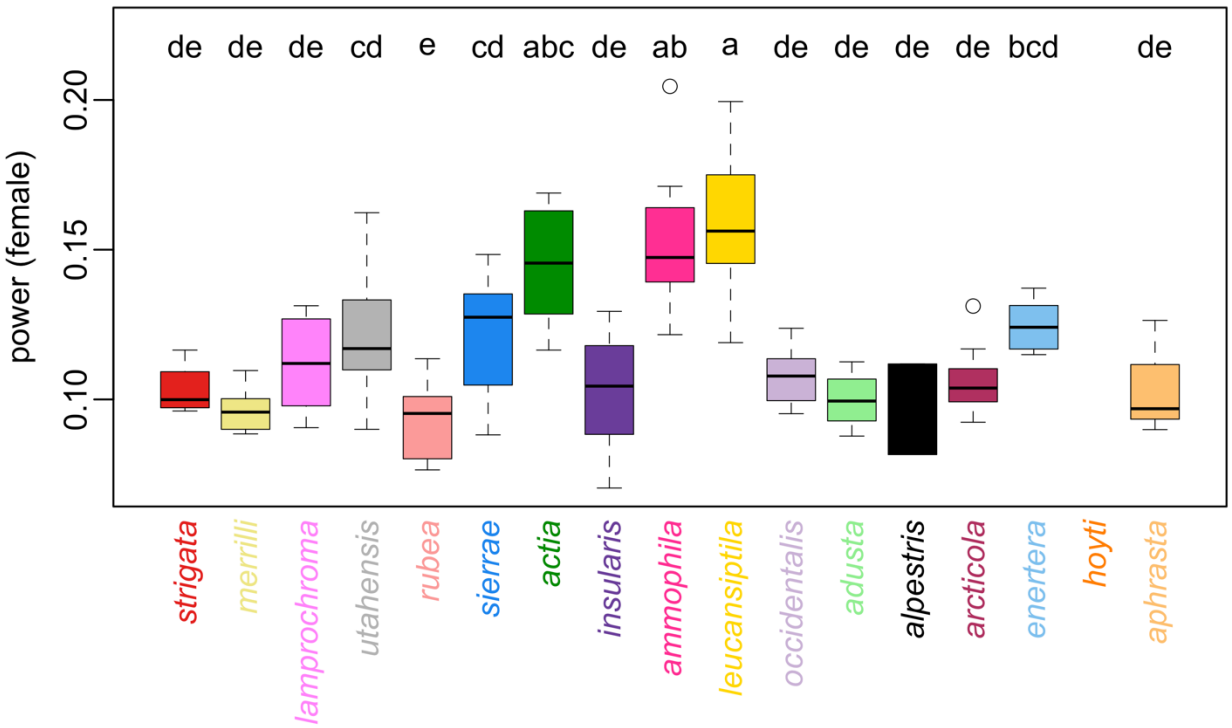

Supplementary Figure S12: Boxplot showing interquartile ranges and variation in power (patterning) among females of different subspecies of Horned Larks. Letters above each plot show the output of a posthoc Tukey's pairwise comparison. Circles represent outliers.

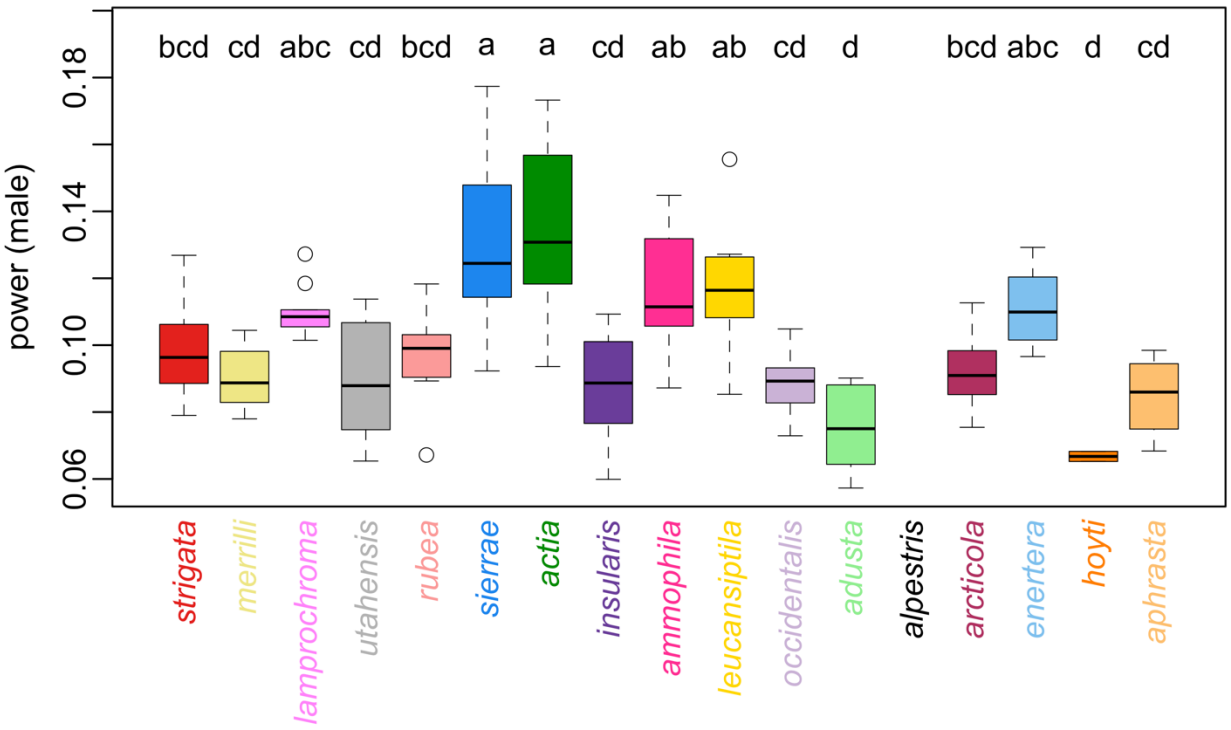

Supplementary Figure S13: Boxplot showing interquartile ranges and variation in power (patterning) among males of different subspecies of Horned Larks. Letters above each plot show the output of a posthoc Tukey's pairwise comparison. Circles represent outliers.

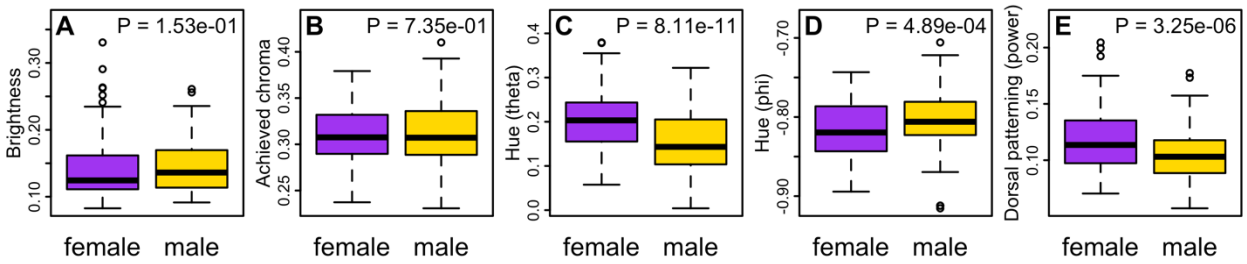

Supplementary Figure S14: Box plots illustrating differences in plumage characters between female and male Horned Larks. P values are taken from the full models in which sex is included as a main effect alongside soil brightness, soil redness, soil granularity, aridity, temperature, and years since collection.

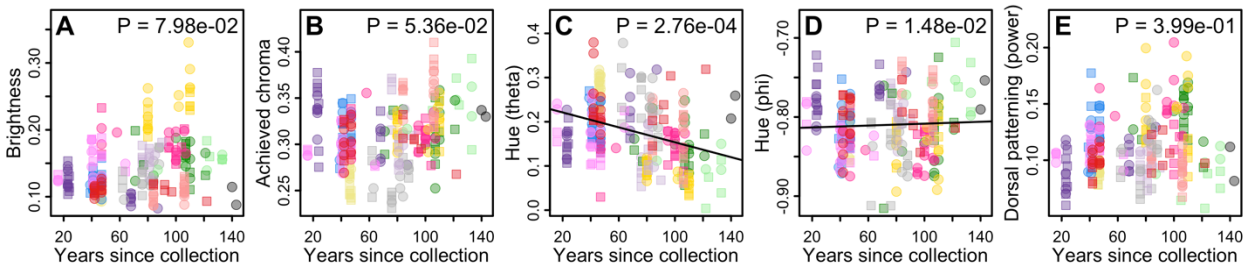

Supplementary Figure S15: Scatterplots showing each plumage metric considered in this study alongside the years since collection for each specimen. P values are taken from the full models in which sex is included as a main effect alongside soil brightness, soil redness, soil granularity, aridity, temperature, and sex. Trend lines are drawn when $P < 0.05$.

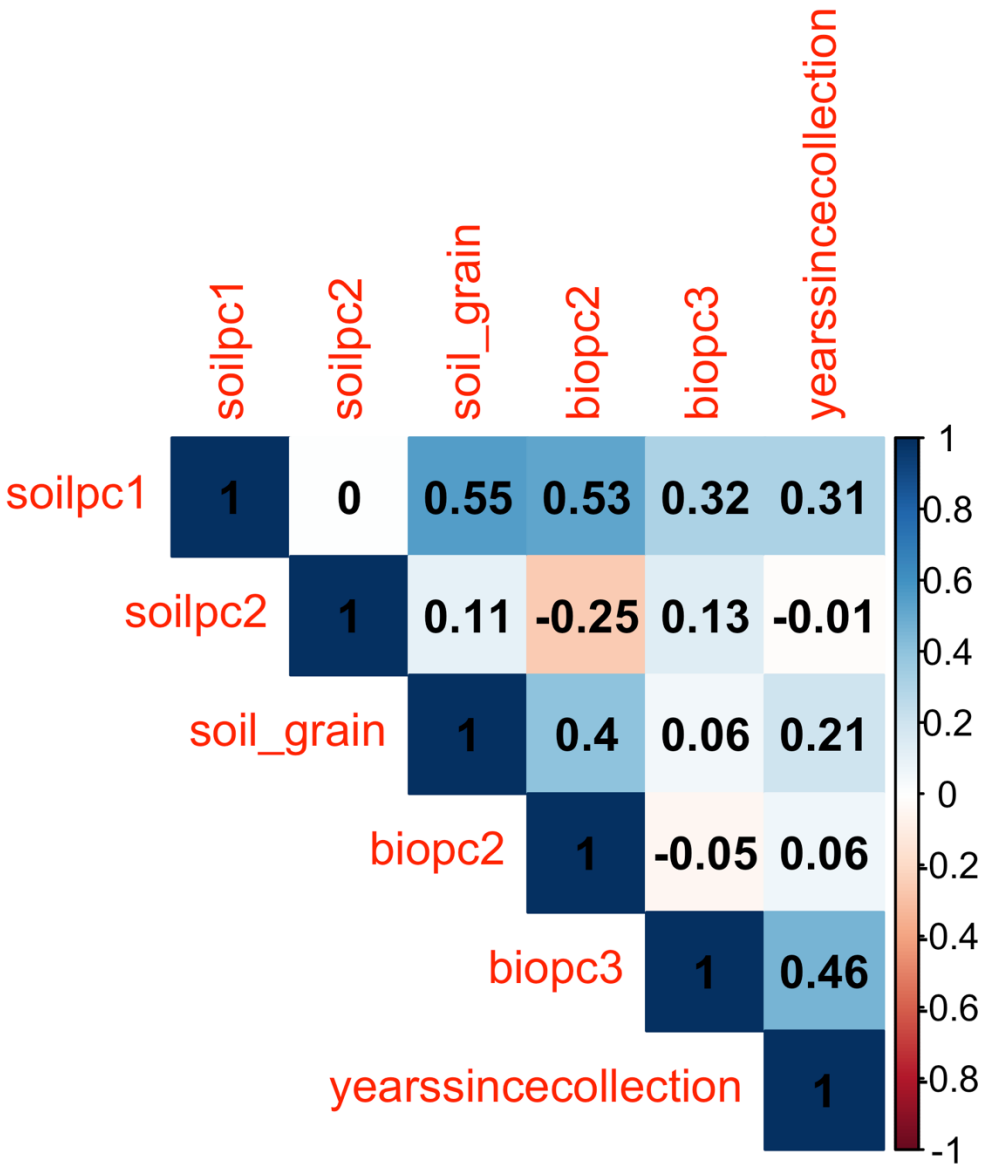

Supplementary Figure S16: Correlation plot showing pair-wise correlation values between predictor variables included in our linear models of plumage-environment associations. Numbers within each box correspond to r^2 values between each pair of variables.

Supplementary Table S1: Voucher information for 270 individuals of Horned Lark (*Eremophila alpestris*) included in this study.

Subspecies	MVZ catalog number	Sex	Year	Month	Day	Country	State / Province	Locality	Longitude	Latitude
actia	3667	male	1908	05	26	USA	California	Chula Vista	32.64	-117.083
actia	3471	female	1908	04	06	USA	California	Nat'l City	32.675	-117.109
actia	3472	female	1908	04	06	USA	California	Nat'l City	32.675	-117.109
actia	3473	female	1908	04	06	USA	California	Nat'l City	32.675	-117.109
actia	3479	male	1908	04	10	USA	California	False Bay	32.808	-117.267
actia	19488	male	1911	04	30	USA	California	Earlimart	35.882	-119.271
actia	19496	female	1911	05	03	USA	California	Earlimart	35.882	-119.271
actia	19486	male	1911	04	24	USA	California	Tipton	36.06	-119.311
actia	19487	female	1911	04	24	USA	California	Tipton	36.06	-119.311
actia	29155	female	1918	06	27	USA	California	"""Hayes Station"", 19 mi SW Mendota"	36.676	-120.611
actia	64599	female	1934	03	19	USA	California	2 mi SW Friant	36.965	-119.728
actia	90619	male	1941	05	19	USA	California	Santa Cruz	36.975	-122.007
actia	120329	female	1947	03	07	USA	California	Santa Cruz	36.986	-122.02
actia	120330	male	1947	03	07	USA	California	Santa Cruz	36.986	-122.02
actia	19481	male	1911	03	21	USA	California	Los Banos	37.061	-120.848
actia	19482	female	1911	03	23	USA	California	Los Banos	37.061	-120.848
actia	19483	male	1911	03	23	USA	California	Los Banos	37.061	-120.848
actia	19484	male	1911	03	23	USA	California	Los Banos	37.061	-120.848
actia	116808	male	1897	03	22	USA	California	San Jose	37.324	-121.89
actia	116809	female	1897	03	22	USA	California	San Jose	37.324	-121.89
adusta	10234	male	1896	05	24	USA	Arizona	Huachuca Mts.	31.489	-110.407
adusta	10235	female	1896	06	30	USA	Arizona	Huachuca Mts.	31.489	-110.407
adusta	24483	male	1913	10	05	USA	Arizona	Fort Huachuca	31.553	-110.347
adusta	5433	male	1885	02	03	USA	Arizona	Fort Huachuca	31.553	-110.347
adusta	5434	male	1885	02	11	USA	Arizona	Fort Huachuca	31.553	-110.347
adusta	5435	female	1885	02	03	USA	Arizona	Fort Huachuca	31.553	-110.347
adusta	5436	female	1885	02	03	USA	Arizona	Fort Huachuca	31.553	-110.347

adusta	78852	male	1894	05	24	USA	Arizona	Willcox	32.253	-109.831
adusta	58954	female	1931	08	30	USA	New Mexico	Horse Camp, Victoria Cattle Co., Animas Valley	31.612	-108.871
alpestris	63384	female	1875	03	27	USA	Massachusetts	Swampscott	42.47	-70.91
alpestris	63386	female	1878	03	16	USA	Massachusetts	Swampscott	42.47	-70.91
ammophila	140817	female	1960	04	12	USA	California	Pinto Basin	33.936	-115.69
ammophila	24550	male	1914	03	20	USA	California	Victorville, Mohave River	34.536	-117.29
ammophila	29166	male	1918	03	14	USA	California	Mohvave	35.053	-118.171
ammophila	29169	female	1918	03	14	USA	California	Mohave	35.053	-118.171
ammophila	29170	female	1918	03	14	USA	California	Mohave	35.053	-118.171
ammophila	29172	male	1918	03	15	USA	California	Mohave	35.053	-118.171
ammophila	29173	male	1918	03	15	USA	California	Mohave	35.053	-118.171
ammophila	29177	female	1918	03	15	USA	California	Mojave	35.053	-118.171
ammophila	82393	female	1923	04	23	USA	California	Taft	35.142	-119.456
ammophila	82394	male	1923	04	24	USA	California	Taft	35.146	-119.456
ammophila	102726	female	1923	05	06	USA	California	Buena Vista Lake	35.188	-119.287
ammophila	102727	male	1923	04	29	USA	California	Buena Vista Lake	35.194	-119.3
ammophila	19502	female	1911	05	23	USA	California	7 mi SE Simmler, Carrizo Plains	35.279	-119.902
ammophila	29153	male	1918	04	17	USA	California	2 mi N Edison Station	35.375	-118.878
ammophila	22501	male	1912	04	28	USA	California	Keeler	36.489	-117.87
ammophila	22502	female	1912	04	28	USA	California	Keeler	36.489	-117.87
ammophila	162726	male	1971	05	22	USA	Nevada	Send Sarcobatus Flat, 7 mi W, 2 mi S Springdale	37.001	-116.881
ammophila	162727	male	1971	05	22	USA	Nevada	Send Sarcobatus Flat, 7 mi W, 2 mi S Springdale	37.001	-116.881
ammophila	162729	female	1971	05	22	USA	Nevada	Send Sarcobatus Flat, 7 mi W, 2 mi S Springdale	37.001	-116.881
ammophila	162730	female	1971	05	22	USA	Nevada	Send Sarcobatus Flat, 7 mi W, 2 mi S Springdale	37.001	-116.881
aphrasta	152933	male	1964	05	02	Mexico	Chihuahua	Ojo Laguna	29.462	-106.33
aphrasta	152934	female	1964	05	02	Mexico	Chihuahua	Ojo Laguna	29.462	-106.33
aphrasta	143776	male	1961	09	02	Mexico	Chihuahua	Ojo de Laguna, 25 mi S Gallego	29.48	-106.402
aphrasta	139540	female	1959	06	21	Mexico	Chihuahua	Sierra del Nido, Canon del Alamo	29.485	-106.77
aphrasta	139544	male	1959	06	21	Mexico	Chihuahua	Sierra del Nido, Canon del Alamo	29.485	-106.77
aphrasta	139545	male	1959	06	21	Mexico	Chihuahua	Sierra del Nido, Canon del Alamo	29.485	-106.77

aphrasta	139546	female	1959	06	21	Mexico	Chihuahua	Sierra del Nido, Canon del Alamo	29.485	-106.77
arcticola	158332	male	1960	05	22	USA	Alaska	9 mi ESE Cape Thompson	68.087	-165.578
arcticola	158334	female	1960	05	29	USA	Alaska	9 mi ESE Cape Thompson	68.087	-165.578
arcticola	158335	male	1960	05	29	USA	Alaska	9 mi ESE Cape Thompson	68.087	-165.578
arcticola	158337	female	1960	05	29	USA	Alaska	9 mi ESE Cape Thompson	68.087	-165.578
arcticola	158333	male	1961	05	28	USA	Alaska	6 mi ESE Cape Thompson	68.1	-165.767
arcticola	102623	male	1888	04	17	Canada	British Columbia	Chilliwack	49.175	-121.942
arcticola	102618	female	1919	08	28	Canada	British Columbia	Pearson Mt., Headwaters Keremeos Cr.	49.179	-119.776
arcticola	102612	female	1925	10	14	Canada	British Columbia	Vancouver Island, Comox	49.683	-124.933
arcticola	102614	female	1925	12	17	Canada	British Columbia	Vancouver Island, Comox	49.683	-124.933
arcticola	102604	male	1930	03	30	Canada	British Columbia	Okanagan Landing	50.233	-119.35
arcticola	102608	male	1929	09	07	Canada	British Columbia	Okanagan Landing	50.233	-119.35
arcticola	102610	female	1929	09	25	Canada	British Columbia	Okanagan Landing	50.233	-119.35
arcticola	42658	female	1921	10	04	Canada	British Columbia	Okanagan Landing	50.233	-119.35
arcticola	42659	female	1921	10	04	Canada	British Columbia	Okanagan Landing	50.233	-119.35
arcticola	82368	female	1913	09	30	Canada	British Columbia	Okanagan Landing	50.233	-119.35
arcticola	102600	female	1920	05	15	Canada	British Columbia	Masset, Graham Island, Queen Charlotte Islands	54.017	-132.15
arcticola	102601	male	1920	05	15	Canada	British Columbia	Masset, Graham Island, Queen Charlotte Islands	54.017	-132.15
arcticola	102593	male	1924	06	19	Canada	British Columbia	Atlin	59.567	-133.7
arcticola	102594	male	1924	07	08	Canada	British Columbia	Atlin	59.567	-133.7
arcticola	102596	female	1924	08	07	Canada	British Columbia	Atlin	59.567	-133.7
enertera	59518	male	1931	01	09	Mexico	Baja California	San Augustin	29.922	-114.969
enertera	59563	female	1931	06	03	Mexico	Baja California Sur	Magdalena, Santa Magdalena Id.	24.909	-112.222
enertera	59534	female	1931	05	13	Mexico	Baja California Sur	Hiray, Llano de Hiray	25.344	-111.938
enertera	59535	male	1931	05	13	Mexico	Baja California Sur	Hiray, Llano de Hiray	25.344	-111.938
enertera	59538	female	1931	05	13	Mexico	Baja California Sur	Hiray, Llano de Hiray	25.344	-111.938
enertera	59539	female	1931	05	13	Mexico	Baja California Sur	Hiray, Llano de Hiray	25.344	-111.938
enertera	59541	male	1931	05	13	Mexico	Baja California Sur	Hiray, Llano de Hiray	25.344	-111.938
enertera	59542	male	1931	05	14	Mexico	Baja California Sur	Hiray, Llano de Hiray	25.344	-111.938
enertera	59543	female	1931	05	14	Mexico	Baja California Sur	Hiray, Llano de Hiray	25.344	-111.938

enertera	59545	female	1931	05	14	Mexico	Baja California Sur	Hiray, Llano de Hiray	25.344	-111.938
enertera	59552	male	1931	05	14	Mexico	Baja California Sur	Hiray, Llano de Hiray	25.344	-111.938
enertera	59558	male	1931	05	15	Mexico	Baja California Sur	Hiray, Llano de Hiray	25.344	-111.938
enertera	59559	male	1931	05	15	Mexico	Baja California Sur	Hiray, Llano de Hiray	25.344	-111.938
enertera	59560	female	1931	05	15	Mexico	Baja California Sur	Hiray, Llano de Hiray	25.344	-111.938
hoyti	82371	male	1922	03	14	Canada	British Columbia	Okanagan Landing	50.233	-119.35
hoyti	73374	male	1936	06	23	Canada	Manitoba	Churchill	58.769	-94.165
insularis	177000	male	1995	04	13	USA	California	Santa Catalina Id., 1.25 mi N Little Harbor	33.403	-118.477
insularis	177001	male	1995	04	13	USA	California	Santa Catalina Id., 1.25 mi N Little Harbor	33.403	-118.477
insularis	177002	female	1995	04	13	USA	California	Santa Catalina Id., 1.25 mi N Little Harbor	33.403	-118.477
insularis	177003	female	1995	04	13	USA	California	Santa Catalina Id., 1.25 mi N Little Harbor	33.403	-118.477
insularis	177004	male	1995	04	13	USA	California	Santa Catalina Id., 1.25 mi N Little Harbor	33.403	-118.477
insularis	177005	male	1995	04	13	USA	California	Santa Catalina Id., 1.25 mi N Little Harbor	33.403	-118.477
insularis	177006	female	1995	04	13	USA	California	Santa Catalina Id., 1.25 mi N Little Harbor	33.403	-118.477
insularis	176999	female	1995	04	14	USA	California	Santa Catalina Id., 2.5 mi N Little Harbor	33.42	-118.478
insularis	177009	male	1995	04	14	USA	California	W end Santa Catalina Id., 1 mi S and 2 mi E Silver Pk.	33.445	-118.533
insularis	177010	female	1995	04	14	USA	California	W end Santa Catalina Id., 1 mi S and 2 mi E Silver Pk.	33.445	-118.533
insularis	174005	male	1994	04	30	USA	California	W end Santa Cruz Id., Canada de Los Sauces	34.008	-119.848
insularis	174006	male	1994	04	30	USA	California	W end Santa Cruz Id., Canada de Los Sauces	34.008	-119.848
insularis	58402	female	1931	05	23	USA	California	S slope Mt.Diablo, Santa Cruz Island	34.026	-119.783
insularis	120124	female	1950	03	07	USA	California	Forney Cove, Santa Cruz Id.	34.059	-119.918
insularis	120125	male	1950	03	07	USA	California	Forney Cove, Santa Cruz Id.	34.059	-119.918
insularis	120127	male	1950	03	07	USA	California	Forney Cove, Santa Cruz Id.	34.059	-119.918
insularis	120131	female	1950	03	08	USA	California	Forney Cove, Santa Cruz Id.	34.059	-119.918
insularis	120132	female	1950	03	08	USA	California	Forney Cove, Santa Cruz Id.	34.059	-119.918
insularis	120133	female	1950	03	08	USA	California	Forney Cove, Santa Cruz Id.	34.059	-119.918
insularis	174004	male	1994	04	30	USA	California	W end Santa Cruz Id., Canada de Los Sauces	34.066	-119.907
lamprochroma	132294	female	1954	05	31	USA	California	Cabin Creek, White Mts.	37.713	-118.261
lamprochroma	132295	male	1954	06	02	USA	California	Cabin Creek, White Mts.	37.713	-118.261

lamprochroma	165717	female	1978	06	21	USA	Nevada	Clayton Valley, 7 mi S and 2 mi W Silver Pk.	37.744	-117.59
lamprochroma	165718	female	1978	06	21	USA	Nevada	Clayton Valley, 7 mi S and 2 mi W Silver Pk.	37.744	-117.59
lamprochroma	165720	male	1978	06	21	USA	Nevada	Clayton Valley, 7 mi S and 2 mi W Silver Pk.	37.744	-117.59
lamprochroma	165729	male	1978	06	22	USA	Nevada	Clayton Valley, 7 mi S and 2 mi W Silver Pk.	37.744	-117.59
lamprochroma	165730	female	1978	06	22	USA	Nevada	Clayton Valley, 7 mi S and 2 mi W Silver Pk.	37.744	-117.59
lamprochroma	165396	female	1977	06	28	USA	Nevada	Bald Mt. N slope	38.534	-119.115
lamprochroma	165398	male	1977	06	29	USA	Nevada	Bald Mt. N slope	38.534	-119.115
lamprochroma	165400	female	1977	06	29	USA	Nevada	Bald Mt. N slope	38.534	-119.115
lamprochroma	165401	female	1977	06	29	USA	Nevada	Bald Mt. N slope	38.534	-119.115
lamprochroma	165402	male	1977	06	29	USA	Nevada	Bald Mt. N slope	38.534	-119.115
lamprochroma	162686	male	1971	06	07	USA	Nevada	5.5 mi S and 6 mi E Wellington	38.677	-119.264
lamprochroma	162687	female	1971	06	07	USA	Nevada	5.5 mi S and 6 mi E Wellington	38.677	-119.264
lamprochroma	162689	male	1971	06	07	USA	Nevada	5.5 mi S and 6 mi E Wellington	38.677	-119.264
lamprochroma	162691	male	1971	06	08	USA	Nevada	2 mi N Lobdell summit, Pine Grove Hills	38.68	-119.17
lamprochroma	180084	male	2002	05	30	USA	Nevada	4 mi N and 2 mi E Poodle Mtn., 6000 ft., Buffalo Hills, Washoe Co., Nev.	40.876	-119.617
lamprochroma	180088	male	2002	05	30	USA	Nevada	4 mi N and 2 mi E Poodle Mtn., 6000 ft., Buffalo Hills, Washoe Co., Nev.	40.876	-119.617
lamprochroma	180089	female	2002	05	30	USA	Nevada	4 mi N and 2 mi E Poodle Mtn., 6000 ft., Buffalo Hills, Washoe Co., Nev.	40.876	-119.617
lamprochroma	180090	female	2002	05	30	USA	Nevada	4 mi N and 2 mi E Poodle Mtn., 6000 ft., Buffalo Hills, Washoe Co., Nev.	40.876	-119.617
leucansiptila	8090	female	1909	03	30	USA	California	Coyote Well	32.735	-115.967
leucansiptila	102733	female	1916	03	21	USA	California	near Sand Dunes	33.059	-115.224
leucansiptila	102734	female	1916	03	21	USA	California	near Sand Dunes	33.059	-115.224
leucansiptila	1066	female	1908	04	28	USA	California	Mecca	33.572	-116.073
leucansiptila	854	male	1908	04	15	USA	California	Mecca	33.572	-116.073
leucansiptila	961	male	1908	04	17	USA	California	Mecca	33.572	-116.073
leucansiptila	852	male	1908	04	10	USA	California	Mecca	33.573	-116.067
leucansiptila	853	male	1908	04	15	USA	California	Mecca	33.573	-116.067
leucansiptila	855	male	1908	04	15	USA	California	Mecca	33.573	-116.067
leucansiptila	966	female	1908	04	24	USA	California	Mecca	33.573	-116.067
leucansiptila	74252	female	1938	05	27	USA	California	Providence Mts., head of Cedar Canyon	35.176	-115.398

leucansiptila	74253	female	1938	05	27	USA	California	Providence Mts., head of Cedar Canyon	35.176	-115.398
leucansiptila	74254	female	1938	05	27	USA	California	Providence Mts., head of Cedar Canyon	35.176	-115.398
leucansiptila	74255	male	1938	05	27	USA	California	Providence Mts., head of Cedar Canyon	35.176	-115.398
leucansiptila	74457	male	1938	05	27	USA	California	Providence Mts., head of Cedar Canyon	35.176	-115.398
leucansiptila	74245	male	1938	05	14	USA	California	1 mi E Cima	35.238	-115.481
leucansiptila	74248	male	1938	05	16	USA	California	3/4 mi E Cima	35.238	-115.485
leucansiptila	74249	male	1938	05	16	USA	California	3/4 mi E Cima	35.238	-115.485
leucansiptila	74244	female	1938	05	12	USA	California	Cima	35.238	-115.498
leucansiptila	74251	female	1938	05	18	USA	California	2 mi NNE Cima	35.265	-115.498
merrilli	163234	male	1972	03	30	USA	California	Gazelle 2 mi NW, Cleland Ranch	41.542	-122.546
merrilli	163237	male	1972	03	30	USA	California	Gazelle 2 mi NW, Cleland Ranch	41.542	-122.546
merrilli	163239	female	1972	03	30	USA	California	Gazelle 2 mi NW, Cleland Ranch	41.542	-122.546
merrilli	163242	male	1972	03	30	USA	California	Gazelle 2 mi NW, Cleland Ranch	41.542	-122.546
merrilli	163243	male	1972	03	30	USA	California	Gazelle 2 mi NW, Cleland Ranch	41.542	-122.546
merrilli	163247	female	1972	03	29	USA	California	Yreka 1 1/2 mi E and 4 mi S, Brazie Ranch, Killgore Hills Rd.	41.673	-122.612
merrilli	163249	male	1972	03	29	USA	California	Yreka 1 1/2 mi E and 4 mi S, Brazie Ranch, Killgore Hills Rd.	41.673	-122.612
merrilli	163250	female	1972	03	29	USA	California	Yreka 1 1/2 mi E and 4 mi S, Brazie Ranch, Killgore Hills Rd.	41.673	-122.612
merrilli	163251	female	1972	03	29	USA	California	Yreka 1 1/2 mi E and 4 mi S, Brazie Ranch, Killgore Hills Rd.	41.673	-122.612
merrilli	163254	female	1972	03	29	USA	California	Yreka 1 1/2 mi E and 4 mi S, Brazie Ranch, Killgore Hills Rd.	41.673	-122.612
merrilli	163175	male	1971	04	01	USA	California	Montague 1 mi NW, Airport Field, Shasta View Ranch	41.731	-122.545
merrilli	163176	female	1971	04	01	USA	California	Montague 1 mi NW, Airport Field, Shasta View Ranch	41.731	-122.545
merrilli	163177	male	1971	04	01	USA	California	Montague 1 mi NW, Airport Field, Shasta View Ranch	41.731	-122.545
merrilli	163179	female	1971	04	02	USA	California	Montague 1 mi NW, Airport Field, Shasta View Ranch	41.731	-122.545
merrilli	163180	male	1971	04	02	USA	California	Montague 1 mi NW, Airport Field, Shasta View Ranch	41.731	-122.545
merrilli	163216	male	1972	03	26	USA	California	Montague 1 mi NW, Shasta View Ranch	41.737	-122.54
merrilli	163217	female	1972	03	26	USA	California	Montague 1 mi NW, Shasta View Ranch	41.737	-122.54
merrilli	163218	female	1972	03	26	USA	California	Montague 1 mi NW, Shasta View Ranch	41.737	-122.54
merrilli	163219	male	1972	03	26	USA	California	Montague 1 mi NW, Shasta View Ranch	41.737	-122.54

merrilli	163220	female	1972	03	26	USA	California	Montague 1 mi NW, Shasta View Ranch	41.737	-122.54
occidentalis	67284	female	1934	06	08	USA	Arizona	Big Lake, 20 mi S Springerville	33.889	-109.413
occidentalis	67286	female	1934	06	08	USA	Arizona	Big Lake, 20 mi S Springerville	33.889	-109.413
occidentalis	87783	male	1942	06	12	USA	Arizona	U.S. Highway 89, house Rock Ranch, house Rock Valley	36.718	-111.955
occidentalis	87784	male	1942	06	12	USA	Arizona	U.S. Highway 89, house Rock Ranch, house Rock Valley	36.718	-111.955
occidentalis	87785	male	1942	06	12	USA	Arizona	U.S. Highway 89, house Rock Ranch, house Rock Valley	36.718	-111.955
occidentalis	87786	male	1942	06	12	USA	Arizona	U.S. Highway 89, house Rock Ranch, house Rock Valley	36.718	-111.955
occidentalis	87788	female	1942	06	12	USA	Arizona	U.S. Highway 89, house Rock Ranch, house Rock Valley	36.718	-111.955
occidentalis	149571	female	1963	03	12	Mexico	Chihuahua	Ojo Laguna	29.462	-106.33
occidentalis	149572	male	1963	03	28	Mexico	Chihuahua	Ojo Laguna	29.462	-106.33
occidentalis	82390	male	1928	03	08	USA	New Mexico	Saccatone Cr.	33.155	-108.702
occidentalis	71116	male	1937	03	16	USA	New Mexico	1 mi S Santa Fe	35.672	-105.937
occidentalis	71117	male	1937	03	16	USA	New Mexico	1 mi S Santa Fe	35.672	-105.937
occidentalis	71118	male	1937	03	16	USA	New Mexico	1 mi S Santa Fe	35.672	-105.937
occidentalis	71119	male	1937	03	16	USA	New Mexico	1 mi S Santa Fe	35.672	-105.937
occidentalis	71120	female	1937	03	16	USA	New Mexico	1 mi S Santa Fe	35.672	-105.937
occidentalis	71121	female	1937	03	16	USA	New Mexico	1 mi S Santa Fe	35.672	-105.937
occidentalis	82391	female	1933	05	06	USA	New Mexico	Animas R.	36.822	-107.992
rubea	22710	female	1912	04	09	USA	California	Marysville Buttes, 4 mi NW Sutter	39.201	-121.801
rubea	22711	female	1912	04	09	USA	California	Marysville Buttes, 4 mi NW Sutter	39.201	-121.801
rubea	22714	male	1912	04	09	USA	California	Marysville Buttes, 4 mi NW Sutter	39.201	-121.801
rubea	22707	male	1912	04	05	USA	California	Marysville Buttes, 8 mi NW Sutter	39.239	-121.856
rubea	22708	male	1912	04	04	USA	California	Marysville Buttes, 8 mi NW Sutter	39.239	-121.856
rubea	22709	female	1912	04	04	USA	California	Marysville Buttes, 8 mi NW Sutter	39.239	-121.856
rubea	22719	female	1912	05	28	USA	California	Chambers Ravine, 4 mi N Oroville	39.57	-121.555
rubea	22720	male	1912	05	28	USA	California	Chambers Ravine, 4 mi N Oroville	39.57	-121.555
rubea	22721	female	1912	05	28	USA	California	Chambers Ravine, 4 mi N Oroville	39.57	-121.555
rubea	22722	male	1912	05	28	USA	California	Chambers Ravine, 4 mi N Oroville	39.57	-121.555
rubea	22724	male	1912	05	28	USA	California	Chambers Ravine, 4 mi N Oroville	39.57	-121.555
rubea	22727	female	1912	05	28	USA	California	Chambers Ravine, 4 mi N Oroville	39.57	-121.555

rubea	22729	female	1912	05	28	USA	California	Chambers Ravine, 4 mi N Oroville	39.57	-121.555
rubea	64579	female	1934	03	03	USA	California	Dry Creek, 10 mi NE Oroville	39.582	-121.56
rubea	64581	male	1934	03	03	USA	California	Dry Creek, 10 mi NE Oroville	39.582	-121.56
rubea	64583	male	1934	03	03	USA	California	Dry Creek, 10 mi NE Oroville	39.582	-121.56
rubea	64587	male	1934	03	03	USA	California	Dry Creek, 10 mi NE Oroville	39.582	-121.56
rubea	64590	female	1934	03	03	USA	California	Dry Creek, 10 mi NE Oroville	39.582	-121.56
rubea	64592	male	1934	03	03	USA	California	Dry Creek, 10 mi NE Oroville	39.582	-121.56
rubea	64593	female	1934	03	03	USA	California	Dry Creek, 10 mi NE Oroville	39.582	-121.56
sierrae	165405	female	1977	07	12	USA	California	Kyburz Flat	39.502	-120.236
sierrae	165406	male	1977	07	12	USA	California	Kyburz Flat	39.502	-120.236
sierrae	165408	female	1977	07	12	USA	California	Kyburz Flat	39.502	-120.236
sierrae	165409	female	1977	07	12	USA	California	Kyburz Flat	39.502	-120.236
sierrae	165410	male	1977	07	12	USA	California	Kyburz Flat	39.502	-120.236
sierrae	165411	male	1977	07	12	USA	California	Kyburz Flat	39.502	-120.236
sierrae	165415	male	1977	07	13	USA	California	Kyburz Flat	39.502	-120.236
sierrae	165416	female	1977	07	13	USA	California	Kyburz Flat	39.502	-120.236
sierrae	165417	female	1977	07	13	USA	California	Kyburz Flat	39.502	-120.236
sierrae	165419	male	1977	07	13	USA	California	Kyburz Flat	39.502	-120.236
sierrae	162699	male	1971	06	18	USA	California	8 1/2 mi E Mt.Ingalls, SW Corner of McReynolds Valley	39.97	-120.46
sierrae	162700	female	1971	06	18	USA	California	8 1/2 mi E Mt.Ingalls, SW Corner of McReynolds Valley	39.97	-120.46
sierrae	162701	female	1971	06	18	USA	California	8 1/2 mi E Mt.Ingalls, SW Corner of McReynolds Valley	39.97	-120.46
sierrae	162702	male	1971	06	18	USA	California	8 1/2 mi E Mt.Ingalls, SW Corner of McReynolds Valley	39.97	-120.46
sierrae	162703	male	1971	06	18	USA	California	8 1/2 mi E Mt.Ingalls, SW Corner of McReynolds Valley	39.97	-120.46
sierrae	162704	female	1971	06	18	USA	California	8 1/2 mi E Mt.Ingalls, SW Corner of McReynolds Valley	39.97	-120.46
sierrae	162708	male	1971	06	18	USA	California	8 1/2 mi E Mt.Ingalls, SW Corner of McReynolds Valley	39.97	-120.46
sierrae	162711	female	1971	06	18	USA	California	8 1/2 mi E Mt.Ingalls, SW Corner of McReynolds Valley	39.97	-120.46
sierrae	166913	male	1979	07	10	USA	California	McReynolds Valley, SW Corner	39.986	-120.459
sierrae	166915	female	1979	07	10	USA	California	McReynolds Valley, SW Corner	39.986	-120.459
strigata	46853	male	1926	03	05	USA	Oregon	5 mi N Medford	42.399	-122.874

strigata	160767	female	1971	08	31	USA	Oregon	Agate Reservoir, 4 mi ESE White City	42.413	-122.772
strigata	160768	male	1971	08	31	USA	Oregon	Agate Reservoir, 4 mi ESE White City	42.413	-122.772
strigata	160769	female	1971	08	31	USA	Oregon	Agate Reservoir, 4 mi ESE White City	42.413	-122.772
strigata	160772	female	1971	09	01	USA	Oregon	Agate Reservoir, 4 mi ESE White City	42.413	-122.772
strigata	160773	female	1971	09	01	USA	Oregon	Agate Reservoir, 4 mi ESE White City	42.413	-122.772
strigata	160777	female	1971	09	01	USA	Oregon	Agate Reservoir, 4 mi ESE White City	42.413	-122.772
strigata	164441	male	1976	05	22	USA	Oregon	Agate Reservoir, 4 mi ESE White City	42.413	-122.772
strigata	164443	male	1976	05	22	USA	Oregon	Agate Reservoir, 4 mi ESE White City	42.413	-122.772
strigata	164445	female	1976	05	22	USA	Oregon	Agate Reservoir, 4 mi ESE White City	42.413	-122.772
strigata	164447	female	1976	05	22	USA	Oregon	Agate Reservoir, 4 mi ESE White City	42.413	-122.772
strigata	164450	male	1976	05	22	USA	Oregon	Agate Reservoir, 4 mi ESE White City	42.413	-122.772
strigata	164452	female	1976	05	22	USA	Oregon	Agate Reservoir, 4 mi ESE White City	42.413	-122.772
strigata	164454	female	1976	05	22	USA	Oregon	Agate Reservoir, 4 mi ESE White City	42.413	-122.772
strigata	164457	female	1976	05	22	USA	Oregon	Agate Reservoir, 4 mi ESE White City	42.413	-122.772
strigata	46851	male	1926	01	27	USA	Oregon	3 mi S Eagle Point	42.429	-122.802
strigata	65511	male	1934	05	27	USA	Oregon	8 mi NNE Medford	42.434	-122.815
strigata	65513	male	1934	05	27	USA	Oregon	8 mi NNE Medford	42.434	-122.815
strigata	33529	male	1896	05	27	USA	Oregon	Salem	44.943	-123.034
strigata	82381	male	1921	04	24	USA	Washington	Tacoma	47.253	-122.443
utahensis	134099	male	1956	04	12	USA	Idaho	N of Elba	42.248	-113.561
utahensis	67608	female	1934	06	03	USA	Idaho	10 mi N Riddle	42.332	-116.109
utahensis	67701	male	1934	06	14	USA	Idaho	3.5 mi S Decko	42.468	-113.627
utahensis	134098	male	1956	04	11	USA	Idaho	10 mi N Rupert	42.764	-113.676
utahensis	69181	female	1936	07	25	USA	Idaho	Pahsimeroi Valley, 10 mi S Goldburg	44.241	-113.645
utahensis	69184	female	1936	07	25	USA	Idaho	Pahsimeroi Valley, 10 mi S Goldburg	44.241	-113.645
utahensis	69178	female	1936	07	22	USA	Idaho	Pahsimeroi Valley, 6 mi S Goldburg	44.299	-113.645
utahensis	57430	female	1930	04	22	USA	Nevada	5 mi SE Millett P.O.	38.964	-117.114
utahensis	57431	male	1930	04	22	USA	Nevada	5 mi SE Millett P.O.	38.964	-117.114
utahensis	57432	female	1930	04	23	USA	Nevada	5 mi SE Millett P.O.	38.964	-117.114
utahensis	57441	male	1930	05	13	USA	Nevada	5 mi SE Millett P.O.	38.964	-117.114
utahensis	64678	female	1934	05	19	USA	Nevada	on Lincoln Hwy., 15 mi SE Eureka	39.347	-115.642

utahensis	133192	female	1955	06	11	USA	Nevada	9 mi E Jarbidge Pk.	41.841	-115.216
utahensis	134250	male	1956	06	05	USA	Nevada	4 mi N Jarbidge	41.932	-115.431
utahensis	90359	male	1942	04	12	USA	Utah	10 mi W Salt Lake Airport	40.625	-112.182
utahensis	90360	male	1942	04	12	USA	Utah	10 mi W Salt Lake Airport	40.625	-112.182
utahensis	90361	male	1942	04	12	USA	Utah	10 mi W Salt Lake Airport	40.625	-112.182
utahensis	90362	male	1942	04	12	USA	Utah	10 mi W Salt Lake Airport	40.625	-112.182
utahensis	90365	female	1942	04	18	USA	Utah	10 mi W Salt Lake Airport	40.625	-112.182

Supplementary Table S2: Principal component analysis loadings for plumage data set. The first principal component axis loads positively with brighter and more saturated plumage, while the second loads positively with brighter, more patterned, and less red plumage.

	PC1	PC2	PC3	PC4
Brightness (lumMean)	**0.352**	**0.498**	**0.168**	0.032
Achieved Chroma (r.achieved)	**0.247**	**-0.317**	**-0.865**	**0.123**
Hue (theta)	**-0.896**	0.073	**-0.165**	-0.064
Hue (phi)	0.075	**-0.743**	**0.357**	**-0.409**
Dorsal Patterning (power)	0.075	**0.306**	**-0.262**	**-0.902**

Supplementary Table S3: Principal component analysis loadings for soil color data set. The first principal component axis corresponds to soil brightness, while the second principal component axis corresponds to soil redness.

	PCA 1 Loading	PCA 2 Loading
Red	0.70	0.64
Green	0.57	-0.26
Blue	0.42	-0.72

Supplementary Table S4: Principal component analysis loadings for soil color data set. The first principal component axis corresponds to soil granularity in which higher scores indicate more coarse particles in the soil.

Character	PCA 1 Loading
Coarse fragments (> 2 mm; volume %)	0.16
Sand (mass %)	0.8
Silt (mass %)	-0.49
Clay (mass %)	-0.31

Supplementary Table S5: Loadings of principal component analysis of 19 bioclimatic variables used in linear models to examine associations with solar absorption and models of evaporative cooling costs. Bold values contributed strongly (absolute value of loading above 0.1) to the corresponding principal component axis.

WorldClim Variable	PC1	PC2	PC3
Annual Mean Temperature	0.02	0.06	**0.33**
Mean Diurnal Range	0.00	0.01	0.10
Isothermality	0.00	0.01	0.01
Temperature Seasonality	**-1.00**	-0.02	0.04
Max Temperature of Warmest Month	0.00	0.06	**0.39**
Min Temperature of Coldest Month	0.03	0.05	**0.31**
Temperature Annual Range	-0.03	0.01	0.08
Mean Temperature of Wettest Quarter	0.01	**0.12**	**0.13**
Mean Temperature of Driest Quarter	0.02	0.01	**0.54**
Mean Temperature of Warmest Quarter	0.00	0.07	**0.33**
Mean Temperature of Coldest Quarter	0.03	0.06	**0.32**
Annual Precipitation	0.01	**-0.82**	0.04
Precipitation of Wettest Month	0.01	**-0.14**	0.03
Precipitation of Driest Month	0.00	-0.02	-0.03
Precipitation Seasonality	0.01	0.00	0.03
Precipitation of Wettest Quarter	0.02	**-0.37**	0.06
Precipitation of Driest Quarter	-0.01	-0.06	-0.08
Precipitation of Warmest Quarter	-0.01	-0.05	**-0.20**
Precipitation of Coldest Quarter	0.02	**-0.36**	**0.21**

Table S6. Model selection for climatic covariates and reduction in cooling benefits reveals that cooling benefits were most associated with aridity.

Model	logLik	AICc	ΔAIC	weight
Aridity (PC)	64.32	-122.3	0.00	1
Temperature (PC)	54.01	-101.7	20.61	0
Null	49.88	-95.6	26.67	0
Seasonality (PC)	49.99	-93.6	28.64	0